WATER RESOURCES RESEARCH, VOL. 33, NO. 8, PAGES 1993–2029, AUGUST 1997

A systematic analysis of eight decades of incipient motion studies, with special reference to gravel-bedded rivers

John M. Buffington and David R. Montgomery
Department of Geological Sciences, University of Washington, Seattle

Abstract. Data compiled from eight decades of incipient motion studies were used to calculate dimensionless critical shear stress values of the median grain size, $\tau^*_{c_{50}}$. Calculated $\tau^*_{c_{50}}$ values were stratified by initial motion definition, median grain size type (surface, subsurface, or laboratory mixture), relative roughness, and flow regime. A traditional Shields plot constructed from data that represent initial motion of the bed surface material reveals systematic methodological biases of incipient motion definition; $\tau^*_{c_{50}}$ values determined from reference bed load transport rates and from visual observation of grain motion define subparallel Shields curves, with the latter generally underlying the former; values derived from competence functions define a separate but poorly developed field, while theoretical values predict a wide range of generally higher stresses that likely represent instantaneous, rather than time-averaged, critical shear stresses. The available data indicate that for high critical boundary Reynolds numbers and low relative roughnesses typical of gravel-bedded rivers, reference-based and visually based studies have $\tau^*_{c_{50}}$ ranges of 0.052–0.086 and 0.030–0.073, respectively. The apparent lack of a universal $\tau^*_{c_{50}}$ for gravel-bedded rivers warrants great care in choosing defendable $\tau^*_{c_{50}}$ values for particular applications.

Introduction

Incipient motion of streambeds is a fundamental process with applications to a wide variety of research problems, such as paleohydraulic reconstructions [*Church*, 1978], placer formation [*Komar and Wang*, 1984; *Li and Komar*, 1992], canal design [*Lane*, 1955], flushing flows [*Milhous*, 1990; *Kondolf and Wilcock*, 1992], and assessment of aquatic habitat [*Buffington*, 1995; *Montgomery et al.*, 1996]. Regardless of whether one advocates equal mobility [*Parker et al.*, 1982], selective transport [e.g., *Komar*, 1987a, b], or some other style of sediment movement, most investigators use a standard or modified form of the critical Shields parameter to define incipient motion of a grain size of interest. The Shields parameter, or dimensionless critical shear stress, is defined as $\tau^*_{c_i} = \tau_{c_i}/(\rho_s - \rho)gD_i$, where τ_{c_i} is the critical shear stress at incipient motion for a grain size of interest, D_i; g is the gravitational acceleration; and ρ_s and ρ are the sediment and fluid densities, respectively. Of particular interest for fluvial geomorphologists is determination of dimensionless critical shear stress values of the median grain size, $\tau^*_{c_{50}}$, for high boundary Reynolds numbers characteristic of gravel-bedded streams.

Shields [1936] demonstrated that $\tau^*_{c_{50}}$ of near-uniform grains varies with critical boundary Reynolds number, Re^*_c, and hypothesized on the basis of an analogy with *Nikuradse*'s [1933] findings that $\tau^*_{c_{50}}$ attains a constant value of about 0.06 above $Re^*_c = 489$ (Figure 1). The critical boundary Reynolds number is defined as $Re^*_c = u^*_c k_s/\nu$, where u^*_c is the critical shear velocity for incipient motion ($u^*_c \equiv (\tau_c/\rho)^{1/2}$), k_s is the boundary roughness length scale, and ν is the kinematic viscosity; *Shields* [1936] set $k_s = D_{50}$, the median grain size of the sediment. Although *Shields*' [1936] boundary Reynolds numbers differ from *Nikuradse*'s [1933], the general form of *Shields*' [1936] curve (Figure 1) is quite similar to *Nikuradse*'s [1933] curve, indicating regions of hydraulically smooth, transitional, and rough turbulent flow. The commonly quoted value of $\tau^*_{c_{50}} \approx 0.06$ for rough turbulent flow reflects a single data point within the overall swath of *Shields*' [1936] data (Figure 1).

There have been numerous additions, revisions, and modifications of the Shields curve since its original publication. *Shields* [1936], *Grass* [1970], *Gessler* [1971], and *Paintal* [1971] recognized that incipient motion of a particular grain size is inherently a statistical problem, depending on probability functions of both turbulent shear stress at the bed and intergranular geometry (i.e., friction angles) of the bed material, the latter being controlled by grain shape, sorting, and packing [*Miller and Byrne*, 1966; *Li and Komar*, 1986; *Kirchner et al.*, 1990; *Buffington et al.*, 1992]. Consequently, there is a frequency distribution of dimensionless critical shear stresses for any grain size of interest. Reanalyzing *Shields*' [1936] data and correcting for sidewall effects and form drag, *Gessler* [1971] reported $\tau^*_{c_{50}} \approx 0.046$ for a 50% probability of movement in rough turbulent flow. Without consideration of the probability of movement, *Miller et al.* [1977] arrived at a similar value of $\tau^*_{c_{50}} \approx 0.045$ for rough turbulent flow using compiled flume data from various sources. *Miller et al.* [1977, p. 507] employed data from "flumes with parallel sidewalls where flows were uniform and steady over flattened beds of unigranular, rounded sediments"; sidewall corrections were applied and each source used a consistent definition of incipient motion. Although *Miller et al.* [1977] used carefully selected data to ensure compatibility within their compilation, scrutiny of their data shows use of both uniform and nonuniform sediment mixtures, differing incipient motion definitions between studies, and in some cases bed load transport rates influenced by bed forms.

Using a larger data set and ignoring differences in sediment

Copyright 1997 by the American Geophysical Union.

Paper number 96WR03190.
0043-1397/97/96WR-03190$09.00

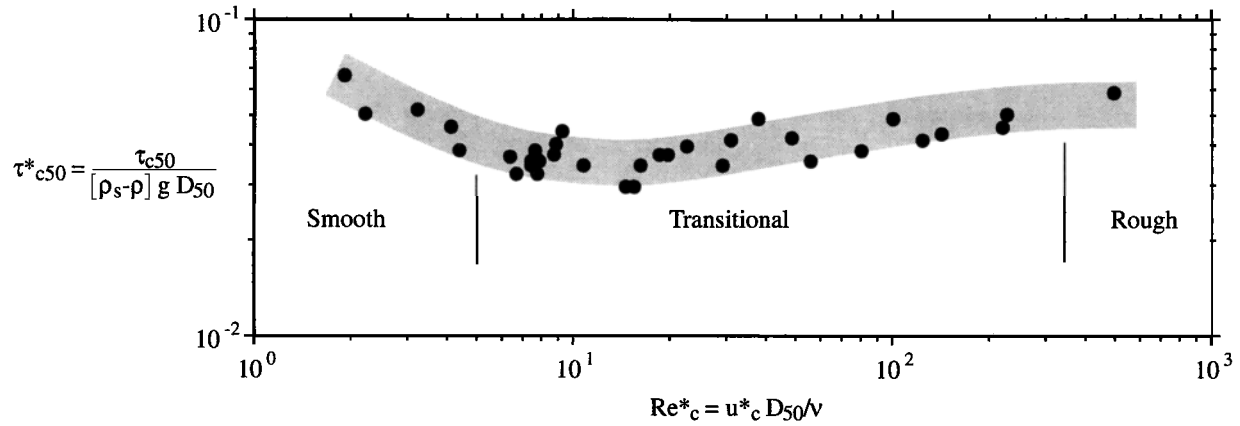

Figure 1. *Shields'* [1936] curve redrafted from *Rouse* [1939].

characteristics, channel roughness, or definition of incipient motion, *Yalin and Karahan* [1979, Figure 5] also report $\tau^*_{c_{50}} \approx 0.045$ for rough turbulent flow. They further demonstrate the existence of a second Shields curve for fully laminar flow, which for the same Re^*_c values behaves differently than the traditional Shields curve derived from turbulent flow with variable hydrodynamic boundary conditions (i.e., smooth, transitional, or rough). The $\tau^*_{c_{50}}$ values reported by *Miller et al.* [1977] and *Yalin and Karahan* [1979] are average values of data sets with considerable scatter; in both studies individual $\tau^*_{c_{50}}$ values for rough turbulent flow range from about 0.02 to 0.065.

Previous compilations of $\tau^*_{c_{50}}$ values combine data derived from quite different experimental conditions and methodologies with little assessment of compatibility. Continued proliferation of incipient motion studies using new definitions of initial motion further complicates comparison and understanding of published studies. Although differences in experimental condition and methodology have been recognized and discussed [e.g., *Tison*, 1953; *Miller et al.*, 1977; *Carson and Griffiths*, 1985; *Lavelle and Mofjeld*, 1987; *Wilcock*, 1988, 1992b], their influence on reported $\tau^*_{c_{50}}$ values has not been well examined. Here we compile eight decades of incipient motion data and stratify calculated $\tau^*_{c_{50}}$ values by (1) initial motion definition, (2) choice of surface, subsurface or laboratory mixture median grain size, (3) relative roughness, and (4) flow regime, providing a systematic reanalysis of the incipient motion literature. We also evaluate the compatibility of different investigative methodologies and interpret the range of reported $\tau^*_{c_{50}}$ values.

Data Compilation and Stratification

All available incipient motion data are summarized in Tables 1a–1e. Values of $\tau^*_{c_{50}}$, critical boundary Reynolds number (Re^*_c), and median grain size (D_{50}) are reported for each source, as well as experimental conditions and dimensionless critical shear stress equations where these are different than *Shields'* [1936]. Where available, the graphic sorting coefficient (σ_g [*Folk*, 1974]), sediment density (ρ_s), and relative roughness (D_{50}/h_c, where h_c is the critical flow height at incipient motion) are also reported. In many cases values of Re^*_c and $\tau^*_{c_{50}}$ (or particular types of $\tau^*_{c_{50}}$, as discussed later) were not reported but could be calculated from the data and equations presented by the author(s); to be consistent with *Shields* [1936], we used $k_s = D_{50}$ when calculating Re^*_c. The graphic sorting coefficient is defined as $(\phi_{84} - \phi_{16})/2$, where ϕ_{84} and ϕ_{16} are the 84th and 16th percentiles of the grain size distribution expressed in units of the phi ($\log_2$) scale. Values of h_c used to determine relative roughness were back-calculated from depth-slope products where sufficient data were reported. Detailed notes regarding both our calculations and the investigative procedures used by each source are presented by *Buffington* [1995] and are abbreviated in the appendix.

The data compiled in Tables 1a–1e are stratified by incipient motion definition. The four most common methods of defining incipient motion are: (1) extrapolation of bed load transport rates to either a zero or low reference value (Table 1a) [e.g., *Shields*, 1936; *Day*, 1980; *Parker and Klingeman*, 1982]; (2) visual observation (Table 1b) [e.g., *Gilbert*, 1914; *Kramer*, 1935; *Yalin and Karahan*, 1979]; (3) development of competence functions that relate shear stress to the largest mobile grain size, from which one can establish the critical shear stress for a given size of interest (Table 1c) [e.g., *Andrews*, 1983; *Carling*, 1983; *Komar*, 1987a]; and (4) theoretical calculation (Table 1d) [e.g., *White*, 1940; *Wiberg and Smith*, 1987; *Jiang and Haff*, 1993].

Dimensionless critical shear stresses determined from the first method are based on critical shear stresses associated with either a zero or low reference transport rate extrapolated from paired shear stress and bed load transport measurements. Values determined from this approach are sensitive to the extrapolation method [cf. *Parker and Klingeman*, 1982; *Diplas*, 1987; *Ashworth and Ferguson*, 1989; *Ashworth et al.*, 1992] and the particular reference transport value that is chosen [*Wilcock*, 1988].

Visual observation, used in the second method, is direct but can be subjective depending on one's definition of how much movement constitutes initial motion [e.g., *Gilbert*, 1914; *Kramer*, 1935; *Neill and Yalin*, 1969; *Wilcock*, 1988]. *Paintal* [1971] argues that there will always be some probability of grain movement as long as there is any fluid motion; hence the threshold of movement becomes a definitional construct [see also *Lavelle and Mofjeld*, 1987]. Standardized definitions of incipient motion have been proposed on the basis of the number of grains in motion, the area of bed observed, and the duration of observation [*Neill and Yalin*, 1969; *Wilcock*, 1988]; however, these definitions have not been widely adopted.

Competence functions, used in the third method, are sensitive to the size and efficiency of the sediment trap, sample size, sampling strategy, availability of coarse grain sizes, and curve-

fitting technique [*Wilcock*, 1992b; *Wathen et al.*, 1995]. Furthermore, the competence method is inappropriate for sediment that exhibits equal mobility, as the competence approach relies on selective transport [*Wilcock*, 1988, 1992b].

The fourth method utilizes simple force balance arguments to predict initial motion thresholds and is sensitive to model parameters such as grain protrusion, packing, and friction angle. In our analysis, $\tau^*_{c_{50}}$ values corresponding to these four methods of measuring incipient motion are symbolized as $\tau^*_{c_{r50}}$ (reference), $\tau^*_{c_{v50}}$ (visual), $\tau^*_{c_{q50}}$ (competence), and $\tau^*_{c_{t50}}$ (theoretical).

Data compiled for each definition of incipient motion are further subdivided by median grain size type (e.g., Table 1a). Values of $\tau^*_{c_{50}}$ have been variously reported in the literature for the median grain size of the surface (D_{50s}), subsurface (D_{50ss}), and laboratory sediment mixture (D_{50m}), the three of which are equal only for uniform-sized sediment; corresponding dimensionless critical shear stresses for these three median grain size types are denoted here as $\tau^*_{c_{50s}}$, $\tau^*_{c_{50ss}}$, and $\tau^*_{c_{50m}}$. Expression of dimensionless critical shear stress in terms of the subsurface grain size distribution was popularized by *Andrews* [1983], who expressed the Shields stress of a given grain size of interest ($\tau^*_{c_i}$) as a power law function of the ratio D_i/D_{50ss}; *Andrews* [1983] found that for his data, D_i/D_{50ss} was better correlated with $\tau^*_{c_i}$ than was D_i/D_{50s} ($r^2 = 0.98$ versus 0.89 [*Andrews*, 1983]). Although expression of bed load transport formulations in terms of D_{50ss} [e.g., *Parker et al.*, 1982] seems reasonable because of the general correspondence of bed load and subsurface grain size distributions [*Milhous*, 1973; *Kuhnle*, 1993a], it is counterintuitive to use the dimensionless critical shear stress of the subsurface to define thresholds of motion and the onset of bed load transport in gravel-bedded channels [e.g., *Andrews*, 1983; *Parker et al.*, 1982]. It is well known that most gravel-bedded rivers are armored and that the surface and subsurface grain size distributions can differ significantly [e.g., *Leopold et al.*, 1964; *Milhous*, 1973]. Analysis of incipient motion of gravel-bedded rivers therefore should employ surface values of critical shear stress. No matter how well the subsurface grain size distribution correlates with the bed load transport size distribution, the initiation of bed load transport is controlled by bed surface grains. Nevertheless, the correspondence of subsurface and transport size distributions indicates that subsurface-based mobility values are appropriate for describing bed load transport beyond incipient motion. Because the difference between subsurface and surface grain size distributions is unpredictable, there is no a priori conversion of subsurface-based incipient motion values to surface ones.

There is currently little recognition in the incipient motion literature of the difference between $\tau^*_{c_{50}}$ values for the various D_{50} types (i.e., $\tau^*_{c_{50s}}$, $\tau^*_{c_{50ss}}$, and $\tau^*_{c_{50m}}$). As such, careful evaluation of reported values is necessary in order to compare and choose appropriate values of $\tau^*_{c_{50}}$. For example, using an Andrews-type power function expressed in terms of a generic median grain size, *Komar* [1987a] reports a generic $\tau^*_{c_{50}}$ value of 0.045 for three gravel channels studied by *Milhous* [1973], *Carling* [1983], and *Hammond et al.* [1984]. It is only upon close inspection of *Komar*'s [1987a] analysis that it becomes apparent that this value represents incipient motion of grain sizes similar or equal to the median subsurface size (note 32, appendix); the corresponding unreported surface values ($\tau^*_{c_{50s}}$) range from 0.021 to 0.027 (Table 1c), roughly half that reported by *Komar* [1987a]. Scaling critical shear stresses by subsurface median grain sizes generally produces $\tau^*_{c_{50}}$ values larger than surface-based ones because of bed surface armoring (compare $\tau^*_{c_{50s}}$ and $\tau^*_{c_{50rs}}$ values of *Parker and Klingeman* [1982], *Wilcock and Southard* [1988], *Kuhnle* [1992], *Andrews and Erman* [1986], *Komar* [1987a], and *Komar and Carling* [1991], given in Tables 1a and 1c).

We emphasize that the dimensionless critical shear stress values reported here are for the median grain size only. Shields parameters of other grain sizes of interest will vary as a function of size-specific friction angle, grain protrusion, and mobility of neighboring grains.

Analysis

Of the 613 dimensionless critical shear stress values compiled in Tables 1a–1e, we examined only those that represent incipient motion of the bed surface, because of their relevance for determining sediment transport thresholds in armored gravel-bedded channels. Subsurface dimensionless critical shear stress values ($\tau^*_{c_{50ss}}$) were removed from the database, as they were all derived from armored channels and thus do not represent initial motion of the streambed surface.

Sorting coefficients (σ_g) were used to establish conditions in which initial motion of laboratory mixtures could be used as a measure of surface mobility (i.e., establishing when $\tau^*_{c_{50m}}$ approximates $\tau^*_{c_{50s}}$). Poorly sorted laboratory sediment mixtures have the potential to exhibit textural response and reworking prior to measurement of incipient motion in both reference-based and visually based studies. Reference-based laboratory studies commonly employ shear stress and bed load transport data collected after attainment of equilibrium conditions of slope, bed form character, and transport rate [e.g., *Gilbert*, 1914; *Shields*, 1936; *Guy et al.*, 1966; *Williams*, 1970; *Wilcock*, 1987], prior to which considerable reworking of the bed surface may occur [e.g., *Wilcock and Southlard*, 1989; *Wilcock and McArdell*, 1993]. Visually based studies also allow varying degrees of water working and sediment transport depending on the specific definition of initial motion employed [e.g., *Kramer*, 1935, *U.S. Waterways Experimental Station* (*USWES*), 1935]. Consequently, the actual surface grain size distribution of initially poorly sorted mixtures may not resemble the original mixture distribution at the time of incipient motion measurement. This causes potentially erroneous results when measured shear stresses for water-worked sediments are combined with unworked mixture distributions to determine dimensionless critical shear stress, as is commonly done in laboratory studies.

Textural response of laboratory mixtures is controlled by relative conditions of transport capacity and sediment supply [e.g., *Dietrich et al.*, 1989; *Kinerson*, 1990; *Buffington*. 1995]. Depending on the direction of textural response, $\tau^*_{c_{50m}}$ values could overestimate or underestimate actual dimensionless critical shear stress values of the surface ($\tau^*_{c_{50s}}$). Mixture median grain sizes will approximate surface median grain sizes only when laboratory sediment mixtures are well sorted, as there is little potential for textural response of a well-sorted bed material. Hence only under these conditions will dimensionless critical shear stresses of the mixture approximate those of the surface. We confined our use of mixture-based studies to those using well-sorted material, where "well sorted" is defined as $\sigma_g \leq 0.5$. Under this definition, some of the laboratory sediment mixtures used by *Shields* [1936] are mixed-grain (Table 1a). Mixture-based studies with unknown σ_g values were not used.

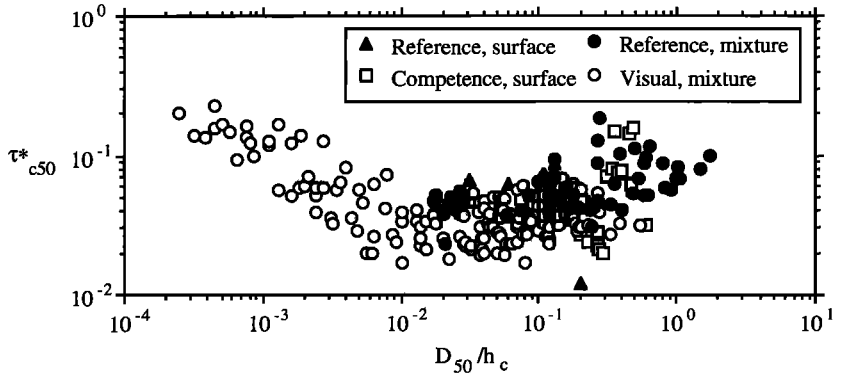

Figure 2. Variation of dimensionless critical shear stress with relative roughness. Only data with known D_{50}/h_c are shown here; all mixture data have $\sigma_{gm} \leq 0.5$.

We further screened the data for relative roughness effects (D_{50}/h_c). *Bathurst et al.* [1983] demonstrated that for a given grain size, $\tau^*_{c_{50}}$ systematically increases with greater relative roughness and that the rate of increase depends on channel slope [see also *Shields*, 1936; *Cheng*, 1970; *Aksoy*, 1973; *Mizuyama*, 1977; *Torri and Poesen*, 1988]. The increase in $\tau^*_{c_{50}}$ with greater relative roughness can be explained through the concept of shear stress partitioning

$$\tau_0 = \tau' + \tau'' + \cdots \tau^n \quad (1)$$

which is predicated on the hypothesis that the total channel roughness and shear stress (τ_0) can be decomposed into linearly additive components (τ', τ'', etc.), each characterizing a particular roughness element [*Einstein and Barbarossa*, 1952; *Engelund*, 1966; *Hey*, 1979, 1988; *Parker and Peterson*, 1980; *Brownlie*, 1983; *Prestegaard*, 1983; *Dietrich et al.*, 1984; *Griffiths*, 1989; *Nelson and Smith*, 1989; *Petit*, 1989, 1990; *Robert*, 1990; *Clifford et al.*, 1992; *Millar and Quick*, 1994; *Shields and Gippel*, 1995]. The effective shear stress (τ') is defined here as that which is available for sediment transport after correction for other roughness elements (i.e., $\tau' = \tau_0 - \tau'' - \cdots \tau^n$).

Based on this concept of shear stress partitioning, greater form drag caused by increased relative roughness (D_{50}/h_c) will decrease the shear stress available at the bed for sediment transport (τ'), resulting in a higher total shear stress (τ_0) required for incipient motion and thus an apparently greater $\tau^*_{c_{50}}$ value. The compiled data demonstrate a general positive correlation between $\tau^*_{c_{50}}$ and D_{50}/h_c over the range $0.01 \leq D_{50}/h_c \leq 2$ (Figure 2). The apparent inverse correlation of $\tau^*_{c_{50}}$ and D_{50}/h_c for $D_{50}/h_c < 0.01$ is a coincident effect of flow regime and is not a relative roughness effect. The compiled data with $D_{50}/h_c < 0.01$ generally have $Re^*_c \leq 20$, which corresponds with the hydrodynamically transitional and smooth portions of the *Shields* [1936] curve for which $\tau^*_{c_{50}}$ is negatively correlated with Re^*_c (Figure 1). It is the association with these low Re^*_c flow regimes, not the relative roughness itself, that causes the apparent inverse correlation of $\tau^*_{c_{50}}$ and D_{50}/h_c for $D_{50}/h_c < 0.01$. Because of the influence of relative roughness on $\tau^*_{c_{50}}$, we restricted our analysis to data with $D_{50}/h_c \leq 0.2$, a value that we chose to be generally representative of gravel-bedded streams. We excluded data from studies with unknown D_{50}/h_c values.

We also excluded data from convergent-wall flume studies because of their apparent incompatibility with those from parallel-wall flumes [*Vanoni et al.*, 1966; *Miller et al.*, 1977]. The above screening results in a database of 325 $\tau^*_{c_{50}}$ values, roughly half of the total compilation.

A traditional Shields plot constructed from data representing initial motion of the bed surface exhibits the expected general form of the original Shields curve but reveals systematic methodological biases of incipient motion definition (Plate 1). Values of $\tau^*_{c_{50}}$ determined from reference bed load transport rates ($\tau^*_{c_{r50}}$) and from visual observation of grain motion ($\tau^*_{c_{v50}}$) define subparallel Shields curves, with the visual data generally underlying the reference data. Reference-based dimensionless critical shear stress values determined from well-sorted laboratory mixtures ($\tau^*_{c_{r50m}}$) and from surface grains of natural channels ($\tau^*_{c_{r50s}}$) dovetail quite well. Dimensionless critical shear stress values derived from competence functions ($\tau^*_{c_{q50s}}$) define a separate but poorly developed field. Although not shown, theoretical values ($\tau^*_{c_{t50r}}$) exhibit no trend in relation to Re^*_c and are widely variable depending on choice of intergranular friction angle and grain protrusion (Table 1d). Furthermore, the theoretical values generally predict high stresses that likely represent instantaneous, rather than time-averaged, critical shear stresses [*Buffington et al.*, 1992]. Scatter within Shields curves has long been attributed to methodological differences between experiments [e.g., *Tison*, 1953; *Miller et al.*, 1977; *Carson and Griffiths*, 1985; *Lavelle and Mofjeld*, 1987], but our reanalysis presents the first comprehensive support for this hypothesis.

The data in Plate 1 are also segregated by flow condition (i.e., fully laminar versus hydraulically smooth, transitional, or rough turbulent flow). We did not limit the laminar data to $D_{50}/h_c \leq 0.2$, as relative roughness effects are unlikely for laminar flow conditions. As demonstrated by *Yalin and Karahan* [1979], two Shields curves are defined for laminar versus turbulent flow conditions over similar Re^*_c values. The lower-angle trend of our compiled laminar curve is similar to that identified by *Yalin and Karahan* [1979].

Despite eight decades of incipient motion studies there remains a lack of $\tau^*_{c_{50}}$ values representative of fully turbulent flow and low relative roughness typical of gravel-bedded rivers (Plate 1). The available data indicate that for such conditions reference-based and visually based studies have $\tau^*_{c_{50}}$ ranges of 0.052–0.086 and 0.030–0.073, respectively (Figure 3). The visual range, however, is rather speculative because of the lack of data for high critical boundary Reynolds numbers.

Scatter within the stratified data sets likely reflects a variety of factors, such as differences in bed material properties (i.e.,

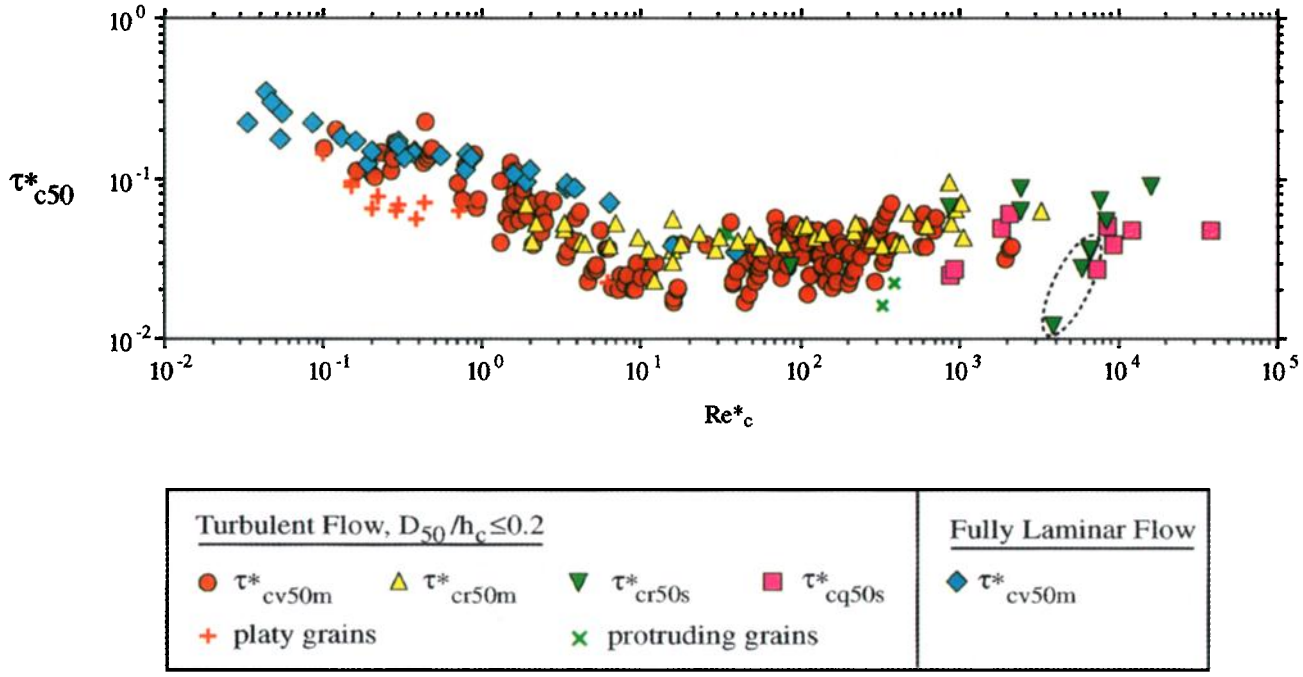

Plate 1. Shields curve for empirical data that represent initial motion of the bed surface material. All mixture-based values have known $\sigma_{gm} \leq 0.5$. Circled triangles are values reported for Oak Creek by *Parker and Klingeman* [1982], *Diplas* [1987], *Wilcock and Southard* [1988], *Parker* [1990], and *Wilcock* [1993]; these values are variations of the same data set (that of *Milhous* [1973]) analyzed using *Parker et al.*'s [1982] definition of incipient motion. The reference-based subcategory of protruding grains indicates significant grain projection and exposure sensu *Kirchner et al.* [1990].

grain sorting, packing, shape, and rounding), neglect of roughness elements (i.e., sidewalls, form drag, etc.), method of shear stress measurement, sampling technique used to characterize grain size distributions (and hence D_{50}), differences in the scale and duration of sediment transport observations, and finer-scale differences in incipient motion definition [e.g., *Wilcock*, 1988]. Differences in bed material properties can either increase or decrease particle mobility. Greater sorting and angularity cause grains to be more resistant to movement and increase $\tau^*_{c_{50}}$ values [*Shields*, 1936; *Miller and Byrne*, 1966; *Li and Komar*, 1986; *Buffington et al.*, 1992]. In contrast, increased sphericity, looser packing, and surfaces with protruding grains increase grain mobility, resulting in lower $\tau^*_{c_{50}}$ values [*Fenton and Abbott*, 1977; *Church*, 1978; *Reid et al.*, 1985; *Li and Komar*, 1986; *Kirchner et al.*, 1990; *Powell and Ashworth*, 1995]. Incipient motion of nonspherical particles is also influenced by their orientation with respect to the downstream flow direction [*Carling et al.*, 1992]. Platy grains (i.e., slates, micaceous flakes, etc.) tend to have very low incipient motion thresholds (Plate 1 and Figure 3) [*Mantz*, 1977].

Neglecting roughness effects (i.e., use of τ_0 rather than τ') causes overestimation of $\tau^*_{c_{50}}$ and introduces a range of scatter that varies with the magnitude of neglected roughness. Form drag caused by relative roughness is a source of scatter that is particularly evident in the visually based data. Many of these data cluster into steeply sloping lineaments (Figure 3b). *Bathurst et al.* [1983] explained this observation as a relative roughness effect, with greater relative roughness causing apparently larger $\tau^*_{c_{50}}$ values, as discussed above. Each lineament in Figure 3b is generally composed of data from a single investigation of a particular bed material [*Gilbert*, 1914; *Liu*, 1935; *Wolman and Brush*, 1961; *Neill*, 1967; *Everts*, 1973]. We examined each lineament and found that most demonstrate the expected positive correlation between D_{50}/h_c and $\tau^*_{c_{50}}$; however, *Neill*'s [1967] data inexplicably show a negative correlation despite Re^*_c values greater than 200. Use of the effective shear stress (τ') rather than the total shear stress (τ_0) in calculating $\tau^*_{c_{50}}$ would likely collapse most of the observed relative roughness lineaments, decreasing $\tau^*_{c_{50}}$.

Although reference-based $\tau^*_{c_{50}}$ values are less variable than visually based ones (Figure 3), potentially large roughness effects caused by bed form drag are commonly neglected in reference studies (Table 1a), which may, in part, explain their larger $\tau^*_{c_{50}}$ values. However, bed form drag also is typically neglected in competence-based studies, which underlie reference-based values (Plate 1). In both reference-based and visually based studies some sidewall corrections are only partial (cf. Tables 1a and 1b). Accurate sidewall correction requires accounting for both differences in bed and wall roughness [e.g., *Vanoni and Brooks*, 1957; *Knight*, 1981; *Flintham and Carling*, 1988; *Shimizu*, 1989] and dissipation of bed shear stress caused by proximity of walls [e.g., *Johnson*, 1942; *Williams*, 1970; *Parker*, 1978; *Knight*, 1981; *Flintham and Carling*, 1988; *Shimizu*, 1989]. Although frequently neglected, the latter correction is of most importance in flume studies, as they typically have narrow width-to-depth ratios (i.e., $W/h < 10$). Partial accounting of sidewall effects can lead to the erroneous conclusion that sidewalls increase the effective bed shear stress [e.g., *Brooks*, 1958; *Wilcock*, 1987; *Kuhnle*, 1993b].

The method used to measure shear stress can also influence $\tau^*_{c_{50}}$. In some instances shear stress is measured as a simple depth-slope product [e.g., *Powell and Ashworth*, 1995], while in other investigations shear stress is estimated from one or more velocity profiles [e.g., *Grass*, 1970; *Ashworth and Ferguson*,

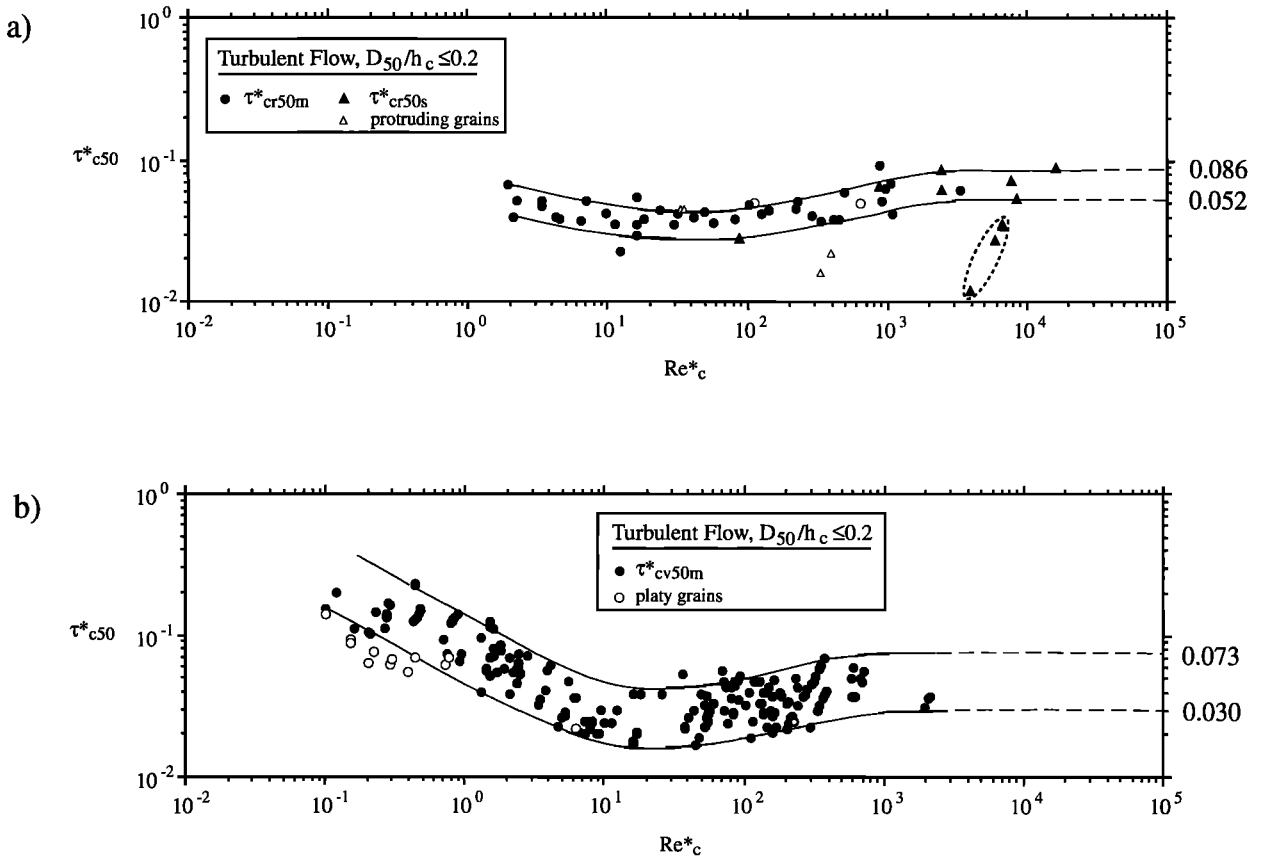

Figure 3. Comparison of (a) reference-based and (b) visually based $\tau^*_{c_{50}}$ data shown in Plate 1. Circled triangles in Figure 3a are discussed in caption to Plate 1. See appendix note 12 regarding open circles of Figure 3a.

1989]. Each of these methods can result in different estimates of shear stress, and thus distinct $\tau^*_{c_{50}}$ values, particularly if shear stress is nonuniform through a study reach.

Use of different sampling techniques to characterize grain size distributions, and hence D_{50}, may also cause some of the observed scatter. The compiled studies use a variety of areal, grid, and volumetric sampling techniques each of which can yield different results [e.g., *Kellerhals and Bray*, 1971; *Diplas and Sutherland*, 1988; *Diplas and Fripp*, 1992; *Fripp and Diplas*, 1993]. Reference-based studies that use *Parker and Klingeman*'s [1982] method are particularly sensitive to grain size sampling technique, as their method employs the proportion of each size class of the grain size distribution.

Although dimensionless critical shear stress is trigonometrically related to bed slope [e.g., *Wiberg and Smith*, 1987] (a factor not accounted for in the traditional Shields equation), its effect on the compiled $\tau^*_{c_{50}}$ values is minimal, as most of the data are derived from experiments with bed slopes less than 0.01. The data of *Bathurst et al.* [1987] and *Mizuyama* [1977] are notable exceptions; however, $\tau^*_{c_{50}}$ values reported for these studies are based on modified Shields stresses that account for both bed slope and bulk friction angle of the sediment (Table 1a).

Use of appropriate k_s values when calculating Re^*_c may reduce some of the observed scatter [e.g., *Ippen and Verma*, 1953]. There have been numerous k_s empiricisms proposed [cf. *Einstein and Barbarossa*, 1952; *Leopold et al.*, 1964; *Kamphuis*, 1974; *Hey*, 1979; *Bray*, 1980], most of which are greater than D_{50s} for heterogeneous bed surfaces; *Whiting and Dietrich* [1990], for example, suggest $k_s = 3D_{84s}$. Although we use $k_s = D_{50s}$ for comparison with historical Shields curves, $k_s = D_{50s}$ is only appropriate for uniformly sized sediment. However, Re^*_c correction using appropriate k_s values will not improve the $\tau^*_{c_{50}}$ uncertainty, which accounts for most of the observed scatter.

Differences in the scale and duration of observation within and between methodologies may also contribute to the scatter of compiled data [e.g., *Neill and Yalin*, 1969; *Fenton and Abbott*, 1977; *Wilcock*, 1988]. For example, the spatial scale of observation in visually based studies varies from the entire bed surface [e.g., *Gilbert*, 1914] to that viewed from a microscope [*White*, 1970]. Similarly, reference- and competence-based studies may employ channel-spanning bed load traps that sample all material passing a cross section [e.g., *Milhous*, 1973] or they may combine several point measures of bed load transport [e.g., *Ashworth and Ferguson*, 1989], representing a smaller scale of observation. Temporal scales of observation also vary among and within methodologies. For example, visually based studies are typically of short duration and made while the channel adjusts to perturbations of slope or hydraulic discharge. In contrast, reference-based studies conducted in flumes employ data collected over long time periods and after attainment of equilibrium conditions of channel morphology and hydraulics. However, reference- and competence-based studies conducted in the field are influenced by nonequilibrium conditions and may require shorter periods of data collection

because of logistics and safety during high flows [e.g., *Ashworth and Ferguson*, 1989; *Wilcock et al.*, 1996]. Differences in spatial and temporal scales of observation can yield different estimates of critical conditions for incipient motion, particularly in channels that exhibit nonuniformities of shear stress, grain size, and bed material properties that cause spatial differences in mobility [e.g., *Powell and Ashworth*, 1995; *Wilcock et al.*, 1996]. Rules for standardizing incipient motion definition and the spatial and temporal scales of observation between investigations have been proposed [e.g., *Neill and Yalin*, 1969; *Yalin*, 1977; *Wilcock*, 1988] but are not widely used. *Wilcock* [1988] proposed a standard definition of incipient motion for mixed-grain sediments that accounts for the number of grains moved, their size and proportion of the grain size distribution, and the area and duration of observation. Even when such rules are applied, channels with identical reach-average shear stresses and grain size distributions may demonstrate different $\tau^*_{c_{50}}$ values because of subreach differences in the spatial variability of shear stress, sediment supply, and bed surface textures (i.e., grain size, sorting, and packing).

Differences of incipient motion definition within each methodology may also contribute to the observed scatter. For example, *Kramer*'s [1935] three definitions of visual grain motion (weak, medium, and general) represent a two-fold difference in $\tau^*_{c_{50}}$ values. Similarly, differences in the choice of dimensionless reference transport rate used to define incipient motion can result in a three-fold variation of reference-based $\tau^*_{c_{50}}$ values [*Paintal*, 1971, Figure 6]. Despite this potential for variation, *Wilcock* [1988] found that reference-based $\tau^*_{c_{50}}$ values determined from the *Parker and Klingeman* [1982] and *Ackers and White* [1973] methods differed by only 5% for the same data set.

Scatter within the reference- and competence-based data may also reflect choice of curve fitting technique [*Diplas*, 1987; *Ashworth and Ferguson*, 1989; *Ashworth et al.*, 1992; *Wathen et al.*, 1995]. In an extreme example, *Paintal* [1971, Figure 8] demonstrates that nonlinear relationships between bed load transport rate and dimensionless shear stress that are mistakenly fit with a linear function can cause up to a five-fold overestimation of reference-based τ^*_{c50} values. In many cases it is difficult to assess or correct differences in curve-fitting technique between investigations due to incomplete documentation of measurements and analysis procedure. The results of *Shields* [1936], in particular, are often used as the standard for comparison, yet *Shields*' [1936] basic measurements and curve fitting technique are unreported, making it difficult to fully assess the causes of discrepancy between *Shields*' [1936] data and those reported by others.

The above influences on $\tau^*_{c_{50}}$ values can be of comparable magnitude and can easily account for the observed scatter of values within methodologies. For example, neglect of roughness effects and natural variation of bed surface characteristics have the potential to cause similar magnitudes of scatter. Variation in particle protrusion and packing can result in an order of magnitude range in $\tau^*_{c_{50}}$ [*Fenton and Abbott*, 1977; *Powell and Ashworth*, 1995], while bed form drag in natural rivers can comprise 10%–75% of the total channel roughness [*Parker and Peterson*, 1980; *Prestegaard*, 1983; *Dietrich et al.*, 1984; *Hey* 1988], indicating a similar range of $\tau^*_{c_{50}}$ variation if bed form resistance is not accounted for. Nonetheless, despite potentially similar sources and/or magnitudes of scatter, the compiled data demonstrate distinct methodological biases (Plate 1).

Discussion

Our reanalysis and stratification of incipient motion values reveal systematic methodological biases and highlight fundamental differences of median grain size type and their associated values of dimensionless critical shear stress. The Shields curve constructed from our data compilation (Plate 1) (1) specifically represents incipient motion of the bed surface, (2) excludes data associated with large relative roughness values that are uncharacteristic of gravel-bedded rivers, and (3) includes for the first time reference- and competence-based $\tau^*_{c_{50}}$ values for surface material ($\tau^*_{c_{r50_s}}$ and $\tau^*_{c_{q50_s}}$). We find that the rough, turbulent flow value of $\tau^*_{c_{50}} \approx 0.045$ reported in previous compilation studies [*Miller et al.*, 1977; *Yalin and Karahan*, 1979] is typical of visually determined mobility thresholds of laboratory mixtures ($\tau^*_{c_{v50m}}$), but underestimates dimensionless critical shear stresses determined from reference transport rates ($\tau^*_{c_{r50m}}$ and $\tau^*_{c_{r50_s}}$) (Figure 3).

Although methodological bias explains much of the scatter in our constructed Shields curve, one is still faced with deciding which investigative method to rely on when choosing a $\tau^*_{c_{50}}$ value. None of the four investigative methods is demonstrably superior; each has its strengths and weaknesses. However, some methods may be more appropriate for particular applications [*Carson and Griffiths*, 1985]. For example, because reference- and competence-based values are derived from bed load transport measures, they may be more well suited to application in bed load transport investigations. Depending on the bed load sampling strategy, reference- and competence-based methods may also integrate differential bed mobility resulting from bed surface textural patches and reach-scale divergence of shear stress and sediment supply and thus may be more appropriate for representing reach-average bed mobility. In contrast, visually based methods typically record local incipient motion and are best applied to mobility studies of discrete bed surface textural patches. Because of methodological biases, care should be taken to choose $\tau^*_{c_{50}}$ values from an investigative method that represents the scale and type of incipient motion needed for one's particular study goals. Conversely, study results should be interpreted in light of the incipient motion method used and the sediment transport processes that it measures. For example, $\tau^*_{c_{50}}$ values from either competence- or reference-based methods could be used to predict reach-average incipient motion, but competence-based values describe motion of the coarsest bed load sizes, whereas reference-based values describe motion of the full bed load distribution; the two methods describe the mobility of different subpopulations of the bed material and may yield different results if equivalent scaling factors are not used [*Wilcock*, 1988].

Of the four methods from which to choose $\tau^*_{c_{50}}$ values, competence-based and theoretically based methods can be excluded because of a paucity of data that precludes confident interpretation of the functional relationship between $\tau^*_{c_{50}}$ and Re^*_c. Nevertheless, the competence-based data define a horizontal band of roughly constant dimensionless critical shear stresses at high Re^*_c values as expected for a Shields-type relationship (Plate 1). Furthermore, this band of data generally lies within the Shields curve defined by visually based methods and systematically underlies the reference-based data (cf. Plate 1 and Figure 3), contrary to expectations that competence values should be greater than reference-based ones due to underrepresentation of coarse grain sizes [*Wilcock*, 1992b].

The fact that some of the data in both methods are derived from the same study sites [*Milhous*, 1973; *Ashworth et al.*, 1992; *Wathen et al.*, 1995] makes this difference between competence- and reference-based approaches credible. For the same study site, competence-based $\tau^*_{c_{50}}$ values are roughly 15%–30% smaller. The systematically lower incipient motion values determined from the competence approach may reflect an inherent bias associated with use of the largest mobile grain size. Larger bed surface grains may have lower mobility thresholds because of greater protrusion and smaller intergranular friction angles [e.g., *Buffington et al.*, 1992]. *Komar and Carling*'s [1991] variant of the competence approach using the median grain size of the load, rather than the maximum grain size, produces $\tau^*_{c_{50}}$ values similar to reference-based ones (Table 1e).

In contrast to theoretically based and competence-based methods, functional relationships between $\tau^*_{c_{50}}$ and Re^*_c are well defined for reference-based and visually based approaches. Both the reference-based and visually based studies exhibit a roughly twofold range in $\tau^*_{c_{50}}$ values for conditions typical of gravel-bedded channels (Figure 3), which represents significant uncertainty in dimensionless critical shear stress. Many bed load transport equations are based on the difference between the applied and critical grain shear stresses raised to some power greater than 1 (see the review by *Gomez and Church* [1989]). Differences between applied and critical shear stresses are typically small in gravel-bedded channels [*Parker et al.*, 1982] because of the approximately bankfull-threshold nature of bed mobility (see the review by *Buffington* [1995]). Consequently, small errors in $\tau_{c_{50}}$ due to uncertainty in $\tau^*_{c_{50}}$ can cause significant errors in calculated bed load transport rates.

Consideration of the sources of scatter and their systematic influence on the reference-based and visually based data provides further guidance in choosing specific $\tau^*_{c_{50}}$ values. In particular, neglect of form drag effects may cause systematic overestimation of $\tau^*_{c_{50}}$ values. It is commonly implied that because flume-based studies of incipient motion employ initially planar bed surfaces they are free of form drag influences caused by bed forms [e.g., *Miller et al.*, 1977]. This is true for the visually based studies, but it is not so for most of the reference-based investigations, such as *Shields*' [1936]. In the visual studies, flow is typically increased gradually until grains are observed to move from a plane-bed surface [e.g., *Kramer*, 1935; *White*, 1970; *Yalin and Karahan*, 1979]. In contrast, most of the reference studies are based on bed load transport data collected after attainment of equilibrium conditions, which in many instances are characterized by the presence of bed forms [e.g., *Gilbert*, 1914; *Shields*, 1936; *Guy et al.*, 1966; *Wilcock and Southard*, 1988]. Because bed form resistance can comprise up to 75% of the total channel roughness [*Hey*, 1988], there is a potentially significant difference between τ' and τ_0, and hence the calculated $\tau^*_{c_{50}}$ value, if bed form roughness is not accounted for. Moreover, it is uncertain whether bed load transport data from surfaces characterized by bed forms can provide a meaningful extrapolation to conditions of initial motion from a lower-regime plane bed, as is commonly intended in laboratory reference-based studies. Although bed form resistance is not an issue in visually based studies, relative roughness effects common to these studies (i.e., lineaments of Figure 3b) may provide an equally important source of form drag and overestimation of $\tau^*_{c_{50}}$ values if not accounted for.

In analyzing incipient motion data it is common practice to fit a single average curve through the scatter of data. However, a Shields curve defined by minimum $\tau^*_{c_{50}}$ values will minimize overestimation of $\tau^*_{c_{50}}$ caused by neglect of form drag resistance in both reference-based and visually based studies (Tables 1a and 1b) and may be more representative of poorly sorted sediments typical of gravel channels. Poorly sorted sediments tend to have lower intergranular friction angles and thus lower incipient motion thresholds [*Buffington et al.*, 1992]. The necessarily narrow range of sorting ($\sigma_g \leq 0.5$) of the mixture data, however, may preclude any meaningful analysis of sorting effects. The $\tau^*_{c_{50}}$ values for rough turbulent flow derived from minimum Shields curves are 0.052 and 0.030 for reference-based and visually based studies, respectively (Figure 3). However, thorough accounting of roughness effects may produce even lower values.

Regardless of whether an average or minimum curve is chosen for the reference-based data, Oak Creek is an outlier (Figure 3a). It does not fit with the expected general form of the traditional Shields curve as defined by the other data. This is somewhat disconcerting, as Oak Creek is believed to be one of the best bed load transport data sets available for natural channels and has been used by many authors as the standard for comparison. Although the issue warrants further investigation, the discrepancy between Oak Creek and the other reference-based data may be due to unaccounted for differences in channel roughness (Table 1a).

Conclusions

Our reanalysis of incipient motion data for bed surface material indicates that (1) much of the scatter in Shields curves is due to systematic biases that investigators should be aware of when choosing and comparing dimensionless critical shear stress values from the literature; and (2) there is no definitive $\tau^*_{c_{50}}$ value for the rough, turbulent flow characteristic of gravel-bedded rivers, but rather there is a range of values that differs between investigative methodologies. Our analysis indicates that less emphasis should be placed on choosing a universal $\tau^*_{c_{50}}$ value, while more emphasis should be placed on choosing defendable values for particular applications, given the observed methodological biases, uses of each approach, and systematic influences of sources of uncertainty associated with different methods and investigative conditions.

Note added in proof. During the time this article was in press we discovered several other referenced-based values similar to those of Oak Creek [see *Andrews*, 1994; *Andrews and Nankervis*, 1995].

Notation

D_{50}, D_{84}, D_i	grain size for which 50%, 84%, and i% of the grains are finer.
D_{50s}, D_{50ss}, D_{50m}, D_{50l}	median grain sizes of the surface, subsurface, laboratory mixture, and bed load.
D_{gs}	geometric mean surface grain size.
g	gravitational constant.
h_c	critical flow depth for incipient motion.
k_s	boundary roughness length scale (equivalent to

Table 1a. Previously Reported $\tau^*_{c_{50}}$ Values: Reference Transport Rate

Source	Note*	Surface Grain Size Distribution: $\tau^*_{c_{r50s}}$	Re^*_c†	Proposed τ^*_c Function Other Than Shields'	D_{50s}, mm	σ_{gs} (ϕ)	ρ_s, kg/m^3	D_{50s}/h_c‡	Experimental Conditions
				Parker and Klingeman [1982] Reference Transport Rate					
Parker and Klingeman [1982]	1	0.035§	6,744	$\tau^*_{c_n} = 0.035(D_i/D_{50s})^{-0.94}$	54	1.09	2850	0.15	natural pool-riffle channel (Oak Creek); no form drag or sidewall correction
Diplas [1987]		0.034§	6,647	$\tau^*_{c_n} = 0.087(D_i/D_{50ss})^{-0.94}$	54	1.09	2850	0.16	same as *Parker and Klingeman* [1982]
From *Wilcock and Southard* [1988]	2								
Milhous [1973]		0.027§	5,923	$\tau^*_{c_n} = 0.073(D_i/D_{50ss})^{-0.98}$	54	1.09	2850	0.20	same as *Parker and Klingeman* [1982]
Ashworth and Ferguson [1989]	3	0.072§	~7,773	$\tau^*_{c_n} = 0.072(D_i/D_{50s})^{-0.65}$	~50	m	2540	0.11	natural pool-riffle channel (Alt Dubhaig), variable sinuosity; sidewall correction implicit
		0.054§	~8,463	$\tau^*_{c_n} = 0.054(D_i/D_{50s})^{-0\,67}$	~57.5	m	2600	0.10	natural pool-riffle channel (River Feshie), mildly braided; sidewall correction implicit
		0.087§	~16,138	$\tau^*_{c_n} = 0.087(D_i/D_{50s})^{-0\,92}$	~69	m	3090	0.13	natural braided channel (Lyngsdalselva); sidewall correction implicit
Parker [1990]		0.034§	6,731	$\tau^*_{c_n} = 0.039(D_i/D_{gs})^{-0.90}$	54	1.02	2850	0.16	same as *Parker and Klingeman* [1982]
Ashworth et al. [1992]		0.061§	2,463	$\tau^*_{c_n} = 0.061(D_i/D_{50s})^{-0\,79}$	24	m	2650	0.06	natural, braided, gravel channel (Sunwapta River); form drag and sidewall correction as in note 3
Kuhnle [1992]		0.065§	869	$\tau^*_{c_n} = 0.086(D_i/D_{50ss})^{-0\,81}$	11.73	0.90	···	0.03	natural channel with mixed gravel and sand bed exhibiting macroscale dunes [*Kuhnle and Bowie*, 1992] (Goodwin Creek); no sidewall or form drag correction
From *Wilcock* [1993]	4								
Milhous [1973]		0.012§	3,949	$\tau^*_{c_n} = 0.033(D_i/D_{50ss})^{-0\,98}$	54	1.09	2850	0.20	same as *Parker and Klingeman* [1982]; *Einstein* [1950] sidewall and form drag correction¶
Wilcock and McArdell [1993]	5	0.028§	88	$\tau^*_{c_n} = 0.028(D_i/D_{50s})^{-0\,45}$, $0.77 \le D_i/D_{50s} \le 17.3$	2.6	2.51	2610	0.12	straight, rectangular flume; variable bedforms; *Einstein* [1950] sidewall and form drag correction¶
Wathen et al. [1995]		0.086§	2,445	$\tau^*_{c_n} = 0.086(D_i/D_{50s})^{-0\,90}$	21.3	~1.6	2650	0.01–0.14	natural pool-riffle channel (Alt Dubhaig), variable sinuosity; no sidewall or form drag correction
				Ackers and White [1973] Reference Transport Rate					
Day [1981]	6	0.035	2,129	···	20	0.92	···	≥0.24–0.41	straight, rectangular flume; plane bed; no sidewall correction
		0.036	2,491	···	22	0.86	···	≥0.28–0.45	as above
				Zero Reference Transport					
Ippen and Verma [1953]		0.045	30	···	2.0	≤0.13	1280	0.23	straight, rectangular flume; plastic test grain placed on fixed plane bed; significant grain projection and exposure;** sidewall effects insignificant

Table 1a. (Continued)

Source	Note*	τ^*_{cr50s}	Re^*_c†	Proposed τ^*_c Function Other Than Shields'	D_{50s}, mm	σ_{gs} (ϕ)	ρ_s, kg/m^3	D_{50s}/h_c‡	Experimental Conditions
				Surface Grain Size Distribution					
		0.044§	33	···	2.0	≤0.13	1280	0.19	as above
		0.045§	35	···	2.0	≤0.13	1280	0.16	as above
Meland and Norrman [1966]	7	0.008§	33	···	2.09	0	2560	≥0.05	straight, rectangular flume; fixed plane bed; glass test grain placed on rhombohedrally packed bed; significant grain projection and exposure;** sidewall correction implicit
		0.022§	390	···	7.76	0	2510	≥0.16	as above
		0.016§	330	···	7.76	0	2510	≥0.16	as above, but with a loose bed
				Laboratory Mixture Grain Size Distribution					
Source	Note*	τ^*_{cr50m}	Re^*_c†	Proposed τ^*_c Function Other Than Shields'	D_{50m}, mm	σ_{gm} (ϕ)	ρ_s, kg/m^3	D_{50m}/h_c‡	Experimental Conditions
				Zero Reference Transport Rate					
From *Shields* [1936]	8								
Gilbert [1914]††		0.059§	489	···	7.01	<0.22	2690?	0.16	straight, rectangular flume; bed form types not reported; partial sidewall correction (?);‡‡ no form drag correction; subrounded grains
		0.051§	227	···	4.94?	<0.26	2690?	0.18	as above
Casey [1935]		0.067§	1.9	···	0.17	0.41	2650	≤0.03	straight, rectangular flume; various bed forms; partial sidewall correction (?); ‡‡ no form drag correction; subangular to rounded grains
		0.052§	3.3	···	0.27	0.42	2650	≤0.04	as above
		0.035§	11	···	0.68	0.16	2650	≤0.10	as above
		0.035§	16	···	0.87	0.17	2650	≤0.12	as above
		0.038§	18	···	0.94	0.19	2650	≤0.05	as above
		0.042§	31	···	1.26	0.20	2650	<0.20?	as above
		0.043§	49	···	1.75	0.19	2650	≤0.10	as above
		0.039§	80	···	2.46	0.22	2650	≤0.10	as above
Kramer [1935]		0.033	6.6	···	0.53	0.81	2700?	≤0.04	straight, rectangular flume; various bed forms; partial sidewall correction (?); ‡‡ no form drag correction; well-rounded grains
		0.039	7.6	···	0.51	0.74	2700?	≤0.04	as above
		0.033	7.8	···	0.55	0.62	2700?	≤0.04	as above
USWES [1935]§§?		0.051§	2.2	···	0.21?	0.32	2650	0.02	straight, rectangular flume; various bed forms; partial sidewall correction (?); ‡‡ no form drag correction
		0.046	4.1	···	0.31?	0.53?	2650	0.02	as above

		0.039§	4.4	···	0.35?	0.37?	2650	0.02	as above
		0.035	7.4	···	0.52?	0.53?	2650	0.03	as above
		0.036	7.4	···	0.51?	0.82?	2650	0.03	as above
		0.036	7.8	···	0.52?	0.53?	2650	0.03	as above
Shields [1936]		0.037§	6.3	···	0.36	0.30	4300	≤0.04?	straight, rectangular flume; various bed form types; form drag and sidewall correction as in note 3; angular barite grains
		0.036§	56	···	1.52	0.35	4200	≤0.04?	as above
		0.042§	124	···	2.46?	0.22	4190	≤0.04?	as above
		0.046§	219	···	3.44	0.16	4200	≤0.04?	as above
		0.044§	142	···	2.76?	0.41	4200	≤0.04?	as above
		0.038	8.8	···	1.56	0.59	1060	≤0.04?	as above, but with angular amber grains; partial sidewall correction;‡‡ no form drag correction
		0.041	8.9	···	1.56	0.59	1060	≤0.04?	as above
		0.045	9.3	···	1.56	0.59	1060	≤0.04?	as above
		0.030§	16	···	0.85	0.23	2700	≤0.04?	as above, but with angular granitic grains
		0.035§	29	···	1.23	0.23	2710	≤0.04?	as above
		0.049§	100	···	2.44	0.23	2690	≤0.04?	as above
		0.030	15	···	1.77?	0.78?	1270	≤0.04?	as above, but with angular coal grains
		0.038	20	···	1.77	0.78	1270	≤0.04?	as above
		0.040	23	···	1.88	0.72	1270	≤0.04?	as above
		0.049	38	···	2.53	0.56	1270	≤0.04?	as above
From *Johnson* [1943]	9								
Gilbert [1914]††	10	0.297	12	···	0.305	<0.09	2690	0.02	straight, rectangular flume; various bed forms; *Einstein* [1942] sidewall correction;¶ no form drag correction; subangular grains
		0.262	15	···	0.375	<0.11	2690	0.02	as above
MacDougall [1933]; River Hydraulics Laboratory, (unpublished report)		0.055§	16	···	0.67	0.38	···	0.03	straight, rectangular flume; bed form types not reported; sidewall correction implicit (?); rounded grains
Chyn [1935]		0.062	14	···	0.60	1.23	···	0.02	as above, but with plane-bed or dune morphology; no form drag correction
		0.044§	23	···	0.83	0.30	···	0.02	as above, but with dunes only
Jorissen [1938]		0.064	16	···	0.62	0.85	2670	0.02	as above, but with planar or rippled bed; no form drag correction
		0.044	24	···	0.92	0.61	2670	0.03	as above
Meland and Norrman [1969]	11	0.047	207	···	3.9	···	2560	<0.08?	straight, rectangular flume; various bed forms; form drag and sidewall correction same as in note 3; glass grains
Paintal [1971]	12	0.050§	638	···	7.95	0.18	2650	0.12	straight, rectangular flume; plane bed (?); *Johnson* [1942] sidewall correction¶
		0.050§	112	···	2.5	0.14	2650	0.02	as above
Sternberg [1971]§§,‖‖		0.048	4.8	···	0.42	1.09	···	$<2 \times 10^{-5}$	sandy marine channel (Pickering Passage) with rippled bed; roughness correction similar to that for note 3
Mizuyama [1977]††,¶¶	13	0.038§ (0.049)	437	$\tau^*_{c_{50m}} = \tau_{c_{50m}}/[(\rho_s - \rho)gD_{50m}(\tan\Phi\cos\theta - \sin\theta)]$	6.4	<0.12	2507	0.12	straight, rectangular flume; bed form type not reported; *Einstein* [1942] sidewall correction;¶ no form drag correction
		0.047 (0.060)	481	as above	6.4	<0.12	2507	0.27	as above
		0.053 (0.066)	507	as above	6.4	<0.12	2507	0.49	as above
		0.042§ (0.041)	1,076	as above	12.0	<0.21	2656	0.12	as above
		0.044 (0.043)	1,096	as above	12.0	<0.21	2656	0.33	as above

Table 1a. (Continued)

Source	Note*	Laboratory Mixture Grain Size Distribution							
		$\tau^*_{c_{r50m}}$	Re^*_c†	Proposed τ^*_c Function Other Than Shields'	D_{50m}, mm	σ_{gm} (ϕ)	ρ_s, kg/m^3	D_{50m}/h_c‡	Experimental Conditions
		0.052(0.049)	1,174	as above	12.0	<0.21	2656	0.59	as above
		0.058 (0.054)	1,227	as above	12.0	<0.21	2656	0.83	as above
		0.067 (0.060)	1,297	as above	12.0	<0.21	2656	1.00	as above
		0.083 (0.072)	1,419	as above	12.0	<0.21	2656	1.04	as above
		0.043 (0.042)	2,637	as above	22.5	<0.08	2490	0.25	as above
		0.051 (0.048)	2,841	as above	22.5	<0.08	2490	0.63	as above
		0.057 (0.053)	2,971	as above	22.5	<0.08	2490	0.90	as above
		0.069 (0.061)	3,199	as above	22.5	<0.08	2490	1.05	as above
		0.079 (0.066)	3,320	as above	22.5	<0.08	2490	1.47	as above
		0.098 (0.077)	3,580	as above	22.5	<0.08	2490	1.73	as above
Pazis and Graf [1977]	14	~0.020	6.2–92	...	0.49–3.02	~u?	2650–1410	<0.02	straight, rectangular flume; sand and plastic grains; bed form types unreported; *Einstein* [1950] sidewall and form drag correction (?)¶
From *Bathurst et al.* [1987] École Polytechnique Fédérale de Lausanne	15	0.052§ (0.036)	905	$\tau^*_{c_{r50m}} = \tau_{c_{r50m}}/[(\rho_s - \rho)gD_{50m}(\tan\Phi\cos\theta - \sin\theta)]$	11.5	~u?	2650	0.08	straight, rectangular flume; various bed forms; *Einstein* [1950] (?) sidewall and form drag (?) correction¶
		0.063§ (0.043)	944	as above	11.5	~u?	2650	0.10	as above
		0.070§(0.048)	1,036	as above	11.5	~u?	2650	0.13	as above
		0.062§ (0.053)	3,231	as above	22.2	0.34	2570	0.12	as above
		0.087 (0.071)	3,436	as above	22.2	0.34	2570	0.27	as above
		0.102 (0.082)	3,621	as above	22.2	0.34	2570	0.39	as above
		0.113 (0.088)	3,753	as above	22.2	0.34	2570	0.50	as above
		0.115 (0.088)	3,886	as above	22.2	0.34	2570	0.65	as above
		0.061 (0.049)	7,976	as above	44.3	~u?	2750	0.35	as above
		0.068 (0.054)	8,366	as above	44.3	~u?	2750	0.53	as above
		0.088 (0.068)	8,714	as above	44.3	~u?	2750	0.59	as above
		0.087 (0.065)	9,131	as above	44.3	~u?	2750	0.79	as above
Bathurst et al. [1979]	16	0.094§ (0.092)	881	as above	8.8	0.42	2629	0.13	straight, rectangular flume; plane-bed or low amplitude bed forms; no form drag or sidewall correction (?)
		0.126 (0.113)	974	as above	8.8	0.42	2629	0.27	as above
		0.185 (0.170)	1,194	as above	8.8	0.42	2629	0.28	as above
		0.095(0.079)	6,198	as above	34	0.44	2629	0.61	as above
Li and Komar [1992]	17	0.048§	3.3	...	0.24	≤0.13	...	0.03	straight, rectangular flume; nonuniform flow; bed form types unreported; no form drag or sidewall correction
				Ackers and White [1973] Reference Transport Rate					
From *Day* [1980] *USWES* [1935]	18	0.050	9.1	...	0.42	0.86	2650	0.02	straight, rectangular flume; various bed forms; no sidewall or form drag correction; subangular to subrounded grains
		0.047	7.3	...	0.44	0.59	2650	0.02	as above, but with angular to subrounded grains

		0.034	189	...	4.10	0.54	2650	0.07	as above, but with subrounded to subangular grains
Day [1980]		0.024	37	...	1.75	2.10	...	0.04	straight, rectangular flume; bed form type not reported; no sidewall or form drag correction
		0.029	34	...	1.55	1.70	...	0.03	as above
Day [1981]	19	0.045	1,025	...	11.3	1.41	...	≥0.24–0.47	straight, rectangular flume; plane bed; no sidewall correction
				Parker and Klingeman [1982] Reference Transport Rate					
Leopold and Emmett [1976, 1977]‖‖	20	0.072	32	$\tau^*_{c_{ri}}=0.072(D_i/D_{50m})^{-0.86}$	1.25	2.8	2650	0.006	natural, dune-ripple channel (East Fork); no sidewall or form drag correction
From *Wilcock and Southard* [1988]									
Day [1980]		0.037	48	$\tau^*_{c_{ri}}=0.037(D_i/D_{50m})^{-0.81}$	1.82	2.09	...	0.03	straight, rectangular flume; bed form type not reported; no form drag or sidewall correction (?)
		0.037	39	$\tau^*_{c_{ri}}=0.037(D_i/D_{50m})^{-0.95}$	1.57	1.73	...	0.03	as above
Dhamotharan et al. [1980]		0.071	108	$\tau^*_{c_{ri}}=0.071(D_i/D_{50m})^{-1.1}$	2.16	1.43	2630	0.07	straight, rectangular flume; bed form type not reported by *Wilcock and Southard* [1988]; no form drag or sidewall correction (?)
Misri et al. [1984]		0.048	101	$\tau^*_{c_{ri}} = 0.048(D_i/D_{50m})^{-1.0}$	2.36	1.05	2650	<0.05	straight, rectangular flume; bed form type not reported; *Einstein* [1950] sidewall and form drag correction¶
		0.042	194	$\tau^*_{c_{ri}} = 0.042(D_i/D_{50m})^{-0.95}$	3.81	1.65	2650	<0.07	as above
		0.037	196	$\tau^*_{c_{ri}} = 0.037(D_i/D_{50m})^{-0\ 92}$	4.00	1.29	2650	<0.07	as above
Wilcock [1987]		0.030	61	$\tau^*_{c_{ri}} = 0.030(D_i/D_{50m})^{-1.0}$	1.83	0.53	2650	0.04	straight, rectangular flume; various bed forms; *Einstein* [1950] sidewall and form drag correction¶
		0.036	67	$\tau^*_{c_{ri}} = 0.036(D_i/D_{50m})^{-0.97}$	1.83	1.06	2650	0.03	as above
		0.023§	12	$\tau^*_{c_{ri}} = 0.023(D_i/D_{50m})^{-0.98}$	0.67	0.29	2650	0.02	as above
		0.037§	332	$\tau^*_{c_{ri}} = 0.037(D_i/D_{50m})^{-1.1}$	5.28	0.20	2650	0.06	straight, rectangular flume; plane bed; *Einstein* [1950] sidewall and form drag correction¶
Wilcock [1992a]	21	0.049	115	$\tau^*_{c_{ri}} = 0.049(D_i/D_{50m})^{-1.04}$	2.55	0.89	...	0.07	straight, rectangular flume; various bed forms; *Einstein* [1950] sidewall and form drag correction;¶ bimodal sediment
		?	?	$\tau^*_{c_{ri}} = 0.017(D_i/D_{50m})^{-1.25}$, $0.27 \le D_i/D_{50m} \le 0.39$; $\tau^*_{c_{ri}} = 0.063(D_i/D_{50m})^{-1.14}$, $2.1 \le D_i/D_{50m} \le 3.1$	2.00	1.65	...	...	as above, but with strongly bimodal sediment; D_{50m} is fictitious, not a size occurring in the mixture
		0.052	19	$\tau^*_{c_{ri}} = 0.52(D_i/D_{50m})^{-0.73}$, $0.7 \le D_i/D_{50m} \le 1.0$; $\tau^*_{c_{ri}} = 0.042(D_i/D_{50m})^{-1.17}$, $5.8 \le D_i/D_{50m} \le 8.3$	0.75	1.67	...	0.01	as above, but D_{50m} is real
Kuhnle [1993b]		0.035	8.4	$\tau^*_{c_{ri}} = 0.035(D_i/D_{50m})^{-1\ 0}$	0.47	2.18	...	0.02	straight, rectangular flume; plane bed or low amplitude bed forms; *Vanoni and Brooks* [1957] sidewall correction¶,***
		0.039§	404	$\tau^*_{c_{ri}} = 0.039(D_i/D_{50m})^{-1.1}$	5.58	0.36	...	0.12	as above
		0.043	8.7	$\tau^*_{c_{ri}} = 0.043(D_i/D_{50m})^{-1\ 1}$, $0.45 \le D_i/D_{50m} \le 2.5$; $\tau^*_{c_{ri}} = 0.019(D_i/D_{50m})^{-0.32}$, $3.6 \le D_i/D_{50m} \le 20.4$	0.47	0.87	...	0.02	as above

Table 1a. (Continued)

Source	Note*	τ^*_{cr50m}	Re^*_c†	Proposed τ^*_c Function Other Than Shields'	D_{50m}, mm	σ_{gm} (ϕ)	ρ_s, kg/m^3	D_{50m}/h_c‡	Experimental Conditions
				Laboratory Mixture Grain Size Distribution					
		0.041	11	$\tau^*_{c_n} = 0.041(D_i/D_{50m})^{-1.0}$, $0.37 \le D_i/D_{50m} \le 3.0$; $\tau^*_{c_n} = 0.035(D_i/D_{50m})^{-0.55}$, $4.2 \le D_i/D_{50m} \le 11.9$	0.57	1.89	···	0.02	as above
		0.045	29	$\tau^*_{c_n} = 0.045(D_i/D_{50m})^{-1.0}$, $0.22 \le D_i/D_{50m} \le 1.2$; $\tau^*_{c_n} = 0.037(D_i/D_{50m})^{-0.42}$, $1.8 \le D_i/D_{50m} \le 7.1$	0.95	2.03	···	0.03	as above
Wilcock and McArdell [1993]	22	0.020	219	$\tau^*_{c_n} = 0.028(D_i/D_{50s})^{-0.45}$, $0.77 \le D_i/D_{50s} \le 17.3$	5.3	2.88	2610	0.16	straight, rectangular flume; variable bed forms; *Einstein* [1950] sidewall and form drag correction¶
				Other Reference Transport Definition					
From *Bridge and Dominic* [1984]									
Gilbert [1914]††		0.040§	4.2	···	0.30	<0.09	2690	0.08	straight, rectangular flume; upper stage plane bed; *Williams* [1970] sidewall correction; subangular river sand
		0.052§	6.9	···	0.38	<0.11	2690	0.13	as above
		0.042§	9.6	···	0.51	<0.26	2690	0.17	as above
		0.030	16	···	0.79	<0.32	2690	0.24	as above
		0.040	145	···	3.17	<0.24	2690	0.24	as above, but lower stage plane bed and subrounded river gravel
		0.041§	286	···	4.94	<0.26	2690	0.19	as above
Williams [1970]		0.040	36	···	1.35	0.20	···	0.40	straight, rectangular flume; upper stage plane bed; *Williams* [1970] sidewall correction
		0.040§	41	···	1.35	0.20	···	0.07	as above, but lower stage plane bed
Guy et al. [1966]		0.040§	2.1	···	0.19	0.45	···	0.02	straight, rectangular flume; upper stage plane bed; no sidewall correction
		0.040	3.3	···	0.28	0.81	···	0.03	as above
		0.040	4.4	···	0.32	0.65	···	0.07	as above
		0.040	22	···	0.93	0.59	···	0.008	as above, but lower stage plane bed

Source	Note*	τ^*_{cr50ss}	Re^*_c†	Proposed τ^*_c Function Other Than Shields'	D_{50ss}, mm	σ_{gss} (ϕ)	ρ_s, kg/m^3	D_{50ss}/h_c‡	Experimental Conditions
				Subsurface Grain Size Distribution					
				Parker and Klingeman [1982] Reference Transport Rate					
Parker and Klingeman [1982]		0.088	2,410	$\tau^*_{c_n} = 0.088(D_i/D_{50ss})^{-0.98}$	20	2.20	2850	0.06	same as *Parker and Klingeman* [1982], first entry of Table 1a
From *Wilcock and Southard* [1988]									
Milhous [1973]		0.073	2,113	$\tau^*_{c_n} = 0.073(D_i/D_{50ss})^{-0.98}$	19.5	2.20	2850	0.07	as above
Kuhnle [1992]		0.086	596	$\tau^*_{c_n} = 0.086(D_i/D_{50ss})^{-0.81}$	8.31	2.77	···	0.02	same as *Kuhnle* [1992], seventh entry of Table 1a
Kuhnle [1993b]		0.089	606	$\tau^*_{c_n} = 0.080(D_i/D_{50ss})^{-0.94}$, $0.04 \le D_i/D_{50m} \le 0.34$; $\tau^*_{c_n} = 0.089(D_i/D_{50ss})^{-0.81}$, $0.67 \le D_i/D_{50m} \le 5.4$	8.31	2.77	···	0.02	as above seventh entry of Table 1a

Note that symbols for similar footnotes may be different in Tables 1a–1e. While most τ^*_{cr50} values are determined from extrapolation of bed load transport rates, some are based on extrapolation of particle or bed form velocity [e.g., *Ippen and Verma*, 1953; *Meland and Norrman*, 1966; *Sternberg*, 1971]. See notation section for symbols not previously defined in text. See respective appendix notes for values in parentheses. Here "u" denotes uniform grain sizes ($\sigma_g \leq 0.5$), and "m" denotes mixed grain sizes ($\sigma_g > 0.5$), where σ_g is the graphic standard deviation defined as $(\phi_{84} - \phi_{16})/2$ [*Folk*, 1974].

*See appendix.

†$Re^*_c = u^*_c D_{50}/\nu$. Most values are back-calculated from reported data. For example, using τ^*_{cr50s} and D_{50s} reported by *Parker and Klingeman* [1982], we calculated τ_{cr50s} from *Shields*' [1936] equation, allowing determination of $u^*_c = (\tau_{cr50s}/\rho)^{0.5}$, and hence Re^*_c, with ν estimated from water temperatures reported by *Milhous* [1973]. Where unreported by the original source, it was assumed that ρ_s and ρ were 2650 and 1000 kg/m^3, respectively, and that $\nu = 10^{-6}$ m^2/s for laboratory and theoretical studies and 1.5×10^{-6} m^2/s for field studies.

‡Where unreported by a source, h_c values are back-calculated from the *Shields* [1936] equation with the τ_c expressed as a depth-slope product ($h_c = \tau^*_c (\rho_s - \rho) D_{50}/\rho_S$, with S determined from the original source, where available). For example, we used the average slope of *Gilbert*'s [1914] 7.01-mm experiments for the first Gilbert entry from *Shields* [1936]; for Gilbert entries from *Bridge and Dominic* [1984] we used the subset of slopes corresponding with plane bed morphologies for each sediment. This procedure may cause overestimation of D_{50}/h_c where depth-slope products have been reduced for roughness effects.

§Used in Plate 1.

‖Reported data are with respect to the geometric mean grain size.

¶Use of the average velocity in the *Einstein* [1942; 1950], *Johnson* [1942] and *Vanoni and Brooks* [1957] equations likely overestimates τ' (see note 3).

**Here we describe grain protrusion in terms of projection and exposure [sensu *Kirchner et al.*, 1990].

††Reported data are with respect to the mean nominal grain diameter. Nominal diameters are assumed equivalent to intermediate grain diameters [*Cui and Komar*, 1984]. Mean and median sizes are similar for near-uniform sediment.

‡‡Sidewall correction for the proximity of walls (i.e., W/h), but not for the difference in wall and bed grain roughness.

§§Reported data are with respect to mean grain sizes. Mean and median grain sizes are assumed similar for near-uniform sediment.

‖‖Reported data are determined from bulk (i.e., surface and subsurface mixture) grain size sampling, treated here as mixture-based values.

¶¶Also given by *Ashida and Bayazit* [1973].

***Sidewall correction for the difference in wall and bed grain roughness but not for the proximity of walls (i.e., W/h).

Table 1b. Previously Reported $\tau^*_{c_{50}}$ Values: Visual Observation

Source	Note*	Surface Grain Size Distribution: $\tau^*_{c_{v50s}}$	Re^*_c†	Proposed τ^*_c Function Other Than Shields'	D_{50s}, mm	σ_{gs} (ϕ)	ρ_s, kg/m^3	D_{50s}/h_c‡	Experimental Conditions
				Various Movement Definitions					
Coleman [1967]	23	0.284 (0.005)	6.2	···	12.7	0	1278	···	straight rectangular flume; sidewall correction implicit; plastic test grain on fixed plane bed of like grains; significant projection and exposure;§ saddle rotation; shear measured with strain gauge; water or sodium carboxymethyl-cellulose fluid medium
		0.284 (0.005)	7.3	···	12.7	0	1278	···	as above
		0.255 (0.004)	7.3	···	12.7	0	1278	···	as above
		0.230 (0.004)	10	···	12.7	0	1278	···	as above
		0.195 (0.004)	13	···	12.7	0	1278	···	as above
		0.166 (0.004)	12	···	12.7	0	1278	···	as above
		0.160 (0.004)	15	···	12.7	0	1278	···	as above
		0.142 (0.004)	19	···	12.7	0	1278	···	as above
		0.121 (0.005)	31	···	12.7	0	1278	···	as above
		0.113 (0.009)	130	···	12.7	0	1278	···	as above
		0.119 (0.011)	160	···	12.7	0	1278	···	as above
		0.129 (0.011)	190	···	12.7	0	1278	···	as above
		0.138 (0.014)	380	···	12.7	0	1278	···	as above

Table 1b. (continued)

Source	Note*	Surface Grain Size Distribution: $\tau^*_{c_{v50s}}$	Re^*_c†	Proposed τ^*_c Function Other Than Shields'	D_{50s}, mm	σ_{gs} (ϕ)	ρ_s, kg/m^3	D_{50s}/h_c‡	Experimental Conditions
		0.123(0.012)	360	···	12.7	0	1278	···	as above
		0.116(0.004)	19	···	12.7	0	7822	···	as above, but with steel test grain
		0.117(0.004)	23	···	12.7	0	7822	···	as above
		0.084(0.004)	43	···	12.7	0	7822	···	as above
		0.098(0.006)	58	···	12.7	0	7822	···	as above
		0.099(0.007)	82	···	12.7	0	7822	···	as above
		0.108(0.010)	140	···	12.7	0	7822	···	as above
		0.107(0.011)	500	···	12.7	0	7822	···	as above
		0.116(0.012)	610	···	12.7	0	7822	···	as above
		0.107(0.011)	1340	···	12.7	0	7822	···	as above
Fenton and Abbott [1977]		0.248	66	···	2.5	0?	···	···	straight rectangular flume; angular polystyrene grain on fixed plane bed of like grains;** sidewall correction implicit; protrusion of −0.20 .
		0.164	54	···	2.5	0?	···	···	as above, but with protrusion of −0.06
		0.085	39	···	2.5	0?	···	···	as above, but with protrusion of 0.30
		0.050	30	···	2.5	0?	···	···	as above
		0.040	27	···	2.5	0?	···	···	as above, but with protrusion of 0.34
		0.149	51	···	2.5	0?	···	···	as above, but with protrusion of 0.04
		0.119	46	···	2.5	0?	···	···	as above, but with protrusion of 0.16
		0.070	35	···	2.5	0?	···	···	as above, but with protrusion of 0.25
		0.072	72	···	2.5	0?	···	···	as above, but with lead-filled test grains and protrusion of 0.34
		0.032	48	···	2.5	0?	···	···	as above, but with protrusion of 0.41
		0.083	78	···	2.5	0?	···	···	as above, but with protrusion of 0.08
		0.107	88	···	2.5	0?	···	···	as above, but with protrusion of 0.05
		0.053	61	···	2.5	0?	···	···	as above, but with protrusion of 0.44
		0.071	70	···	2.5	0?	···	···	as above, but with protrusion of 0.35
		0.076	73	···	2.5	0?	···	···	as above, but with protrusion of 0.16
		0.009	1690	···	38	0	···	0.23	straight rectangular flume; fixed plane bed of wooden grains; table tennis test grains filled with lead shot or polystyrene grains and sand; sidewall correction implicit; protrusion of 0.82
		0.010	1700	···	38	0	···	0.23	as above
		0.010	1760	···	38	0	···	0.36	as above
		0.011	3200	···	38	0	···	0.36	as above
		0.012	3280	···	38	0	···	0.24	as above
Petit [1994]		0.058	1403	$\tau^*_{c_{ui}} = 0.058(D_i/D_{50s})^{-0.66}$	12.8	<0.20?	2650	···	straight rectangular flume; natural grains on plane bed of like grains; *Vanoni and Brooks* [1957] sidewall correction‖,¶
		0.047	3284	$\tau^*_{c_{ui}} = 0.047(D_i/D_{50s})^{-0.73}$	24.2	<0.34?	2650	···	as above
		0.045	6624	$\tau^*_{c_{ui}} = 0.045(D_i/D_{50s})^{-0.81}$	39.2	<0.15?	2650	···	as above
		0.049	2444	$\tau^*_{c_{ui}} = 0.049(D_i/D_{50s})^{-0.68}$	19.6	<0.54?	2650	···	as above, but with fixed bed

Source	Note*	Laboratory Mixture Grain Size Distribution							
		$\tau^*_{c_{v50m}}$	Re^*_c†	Proposed τ^*_c Function Other Than Shields'	D_{50m}, mm	σ_{gm} (ϕ)	ρ_s, kg/m^3	D_{50m}/h_c‡	Experimental Conditions
				"Medium Movement" [Kramer, 1935] or Its Equivalent					
Gilbert [1914]**	24	0.052††	322	···	4.94	<0.26	2690	0.11	straight, rectangular flume; plane bed; *Shimizu* [1989] sidewall correction;‡‡ Subrounded grains
		0.052††	323	···	4.94	<0.26	2690	0.16	as above
		0.069††	372	···	4.94	<0.26	2690	0.15	as above
		0.048††	310	···	4.94	<0.26	2690	0.17	as above
		0.058††	341	···	4.94	<0.26	2690	0.18	as above
		0.046††	304	···	4.94	<0.26	2690	0.12	as above
		0.047††	308	···	4.94	<0.26	2690	0.16	as above
		0.062††	352	···	4.94	<0.26	2690	0.18	as above
		0.053	326	···	4.94	<0.26	2690	0.27	as above
		0.032††	52	···	1.71	<0.48	2690	0.09	as above
		0.057††	69	···	1.71	<0.48	2690	0.20	as above
		0.049††	160	···	3.17	<0.24	2690	0.11	as above
		0.049††	161	···	3.17	<0.24	2690	0.11	as above
		0.060††	587	···	7.01	<0.22	2690	0.08	as above
Kramer [1935]		0.043	8.2	···	0.53	0.81	2700	0.03	straight, rectangular flume; plane bed; *Shimizu* [1989] sidewall correction;‡‡ well-rounded grains
		0.048	8.7	···	0.53	0.81	2700	0.02	as above
		0.039	7.7	···	0.53	0.81	2700	0.02	as above
		0.040	8.0	···	0.53	0.81	2700	0.01	as above
		0.037	7.3	···	0.51	0.74	2700	0.04	as above
		0.037	7.1	···	0.51	0.74	2700	0.02	as above
		0.034	7.0	···	0.51	0.74	2700	0.02	as above
		0.030	6.5	···	0.51	0.74	2700	0.02	as above
		0.035	7.8	···	0.55	0.62	2700	0.04	as above
		0.039	8.2	···	0.55	0.62	2700	0.02	as above
		0.038	7.9	···	0.55	0.62	2700	0.02	as above
		0.037	8.0	···	0.55	0.62	2700	0.01	as above
USWES [1935]		0.052	9.5	···	0.43	0.95	2650	0.01	straight, rectangular flume; plane bed; *Shimizu* [1989] sidewall correction;‡‡ subangular to subrounded river sand
		0.044	8.8	···	0.43	0.95	2650	0.02	as above
		0.052	9.6	···	0.43	0.95	2650	0.02	as above
		0.051	10	···	0.45	0.66	2650	0.01	as above
		0.067	12	···	0.45	0.66	2650	0.01	as above
		0.043	8.0	···	0.48	0.53	2650	0.01	as above, but subrounded to rounded grains
		0.048	9.0	···	0.48	0.53	2650	0.02	as above
		0.049	8.6	···	0.48	0.53	2650	0.02	as above
		0.052	7.8	···	0.44	0.82	2650	0.01	same as above, but angular to subrounded grains
		0.049	7.6	···	0.44	0.82	2650	0.02	as above
		0.063	8.2	···	0.44	0.82	2650	0.02	as above
		0.053	6.6	···	0.40	0.69	2650	0.01	as above, but angular to subangular grains
		0.053	6.7	···	0.40	0.69	2650	0.02	as above
		0.059	7.0	···	0.40	0.69	2650	0.02	as above
		0.048††	5.5	···	0.34	0.37	2650	0.02	as above, but subrounded to subangular grains

Table 1b. (Continued)

Source	Note*	Laboratory Mixture Grain Size Distribution							
		$\tau^*_{c_{v50m}}$	Re^*_c†	Proposed τ^*_c Function Other Than Shields'	D_{50m}, mm	σ_{gm} (ϕ)	ρ_s, kg/m^3	D_{50m}/h_c‡	Experimental Conditions grains
		0.076	5.1	···	0.25	0.53	2650	0.008	as above
		0.038	196	···	4.0	0.56	2650	0.04	as above
		0.042	200	···	4.0	0.56	2650	0.05	as above
		0.045	212	···	4.0	0.56	2650	0.06	as above
		0.074††	2.4	···	0.18	0.32	2650	0.008	as above, but subangular to angular grains
Chang [1939]**		0.061	1.5	···	0.134		2520	0.0008	straight, rectangular flume, and convergent-walled flume; plane bed; *Shimizu* [1989] sidewall correction‡‡
				"General Movement" [Kramer, 1935]					
From *Kramer* [1935]									
Schaffernak [1916]		0.030	41	···	1.5	0.5	2650	···	unreported by *Kramer* [1935], but experimental procedure directly comparable to his [*Kramer*, 1935]
H. Krey (unpublished Elbe experiments report)		0.057	14	···	0.60	0.94	2650	···	as above
		0.060	13	···	0.57	0.69	2650	···	as above
		0.056	15	···	0.63	0.89	2650	···	as above
		0.053	13	···	0.57	0.71	2650	···	as above
		0.034	21	···	0.92	1.20	2650	···	as above, but less comparable [*Kramer*, 1935]
		0.038	14	···	0.67	1.19	2650	···	as above
		0.069	3.2	···	0.21	0.67	2650	···	as above
H. Krey (unpublished report)		0.038	5.8	···	0.38	0.21	2680	···	as above
		0.033	8.8	···	0.53	0.18	2610	···	as above
		0.025	14	···	0.8	0.24	2570	···	as above
Schoklitsch [1914]		0.052	476	···	6.52	0	2600	···	straight, rectangular flume [*Mantz*, 1977]; slate grains (?); experimental procedure less comparable [*Kramer*, 1935]
		0.041	206	···	4.05	0	2600	···	as above
		0.031	75	···	2.26	0	2600	···	as above
		0.022	26	···	1.24	0	2600	···	as above
		0.019	15	···	0.92	0	2600	···	as above
Engels [1932]		0.061	31	···	1.00	1.35	2650	<0.02	meandering, large-scale flume [*Engels and Kramer*, 1932]; plane bed; no correction for sidewalls or channel curvature (?); experimental procedure less comparable [*Kramer*, 1935]

				Other Visual Movement Definition					
From *O'Brien and Rindlaub* [1934] and *Mavis et al.* [1935]									
Ho [1933]		0.015	5	···	0.5	≤0.25	2620	···	straight, rectangular flume; plane bed; no sidewall correction (?); river sand
		0.014	9	···	0.7	≤0.25	2680	···	as above
		0.024	20	···	1.0	≤0.25	2630	···	as above
		0.028	35	···	1.4	≤0.25	2630	···	as above
		0.030	62	···	2.0	≤0.25	2620	···	as above
		0.029	102	···	2.8	≤0.25	2660	···	as above
		0.024	159	···	4.0	≤0.25	2650/2660	···	as above, but uncertain whether grains are river sand or crushed limestone
		0.036	194	···	4.0	≤0.25	2650/2660	···	as above
		0.028	287	···	5.7?	≤0.25	2650/2660	···	as above
		0.028	288	···	5.7	≤0.25	2650/2660	···	as above
From *Mavis et al.* [1937]									
Liu [1935]		0.022††	198	···	4.3	0.31	2660	0.03	straight, rectangular flume; plane bed; *Shimizu* [1989] sidewall correction‡‡
		0.026††	213	···	4.3	0.31	2660	0.05	as above
		0.024††	207	···	4.3	0.31	2660	0.12	as above
		0.032††	235	···	4.3	0.31	2660	0.19	as above
		0.019††	110	···	3.1	0.33	2660	0.04	as above
		0.028††	135	···	3.1	0.33	2660	0.05	as above
		0.029††	137	···	3.1	0.33	2660	0.10	as above
		0.037††	156	···	3.1	0.33	2660	0.16	as above
		0.024††	75	···	2.2	0.35	2660	0.03	as above
		0.028††	82	···	2.2	0.35	2660	0.05	as above
		0.029††	82	···	2.2	0.35	2660	0.10	as above
		0.035††	90	···	2.2	0.35	2660	0.17	as above
		0.022††	37	···	1.4	0.31	2660	0.03	as above
		0.023††	37	···	1.4	0.31	2660	0.06	as above
		0.026††	39	···	1.4	0.31	2660	0.11	as above
		0.030††	43	···	1.4	0.31	2660	0.20	as above
		0.021††	158	···	3.8	0.36	2660	0.03	as above
		0.023††	165	···	3.8	0.36	2660	0.06	as above
		0.033††	198	···	3.8	0.36	2660	0.09	as above
		0.034††	204	···	3.8	0.36	2660	0.17	as above
		0.026††	53	···	1.7	0.45	2660	0.03	as above
		0.028††	55	···	1.7	0.45	2660	0.05	as above
		0.026††	53	···	1.7	0.45	2660	0.11	as above
		0.030‡‡	57	···	1.7	0.45	2660	0.20	as above
White [1940]	25	0.338††	0.043	···	0.21	~u?	···	0.05	straight, rectangular flume; plane bed; no sidewall correction; oil fluid medium; entirely laminar flow
		0.168††	0.30	···	0.90	~u?	···	0.11	as above
		0.180	2.4	···	0.122	~u	···	···	convergent-walled nozzle; plane bed; no sidewall correction; water fluid medium; laminar boundary layer within steady "inviscid" flow
		0.119	33	···	0.90	~u	2600	···	as above, but with turbulent boundary layer
		0.101	480	···	5.6	~u	2600	···	as above
		0.064	35	···	0.71	m	7900	···	as above, but with steel shot grains

Table 1b. (Continued)

Source	Note*	Laboratory Mixture Grain Size Distribution							
		$\tau^*_{c_{v50m}}$	Re^*_c†	Proposed τ^*_c Function Other Than Shields'	D_{50m}, mm	σ_{gm} (ϕ)	ρ_s, kg/m^3	D_{50m}/h_c‡	Experimental Conditions
		0.098	80	···	0.90	~u	2100	···	as above, but with natural grains and fluid medium of air
		0.102	1280	···	5.6	~u	2100	···	as above
Meyer-Peter and Müller [1948]‖‖		0.033††	133	$\tau^*_{c_{v50m}} = [\tau_{c_{v50m}}(Q_b/Q)(n_g/n_b)^{3/2}]/[(\rho_s - \rho)gD_{50m}]$	3.2	<0.12?	2680	0.01	straight, rectangular flume; plane bed or very low amplitude bed forms; form drag and sidewall correction; rounded grains
		0.032††	101	as above	2.7	<0.15?	2680	0.02	as above
		0.037††	183	as above	3.8	<0.16?	2680	0.02	as above
		0.030††	151	as above	3.6	<0.15?	2680	0.01	as above
		0.039††	178	as above	3.66	<0.13?	2680	0.03	as above
		0.040††	179	as above	3.66	<0.13?	2680	0.06	as above
		0.037††	609	as above	8.5	<0.19?	2680	0.06	as above
		0.050††	575	as above	7.4	<0.28?	2680	0.10	as above
		0.047††	686	as above	8.5	<0.23?	2680	0.10	as above
		0.040††	142	as above	3.14	<0.15?	2680	0.13	as above
		0.033††	59	as above	1.86	<0.33?	2680	0.01	as above, but with angular grains
		0.025††	113	as above	3.14	<0.15?	2680	0.01	as above
		0.033††	127	as above	3.1	<0.17?	2680	0.02	as above
		0.038††	176	as above	3.66	<0.13?	2680	0.03	as above
		0.040††	137	as above	3.06	<0.19?	2680	0.02	as above
		0.040††	106	as above	2.58	<0.18?	2680	0.02	as above
		0.048††	119	as above	2.61	<0.20?	2680	0.05	as above
		0.050††	233	as above	4.04	<0.22?	2680	0.05	as above
		0.043††	241	as above	4.34	<0.22?	2680	0.10	as above
		0.043††	81	as above	2.10	<0.16?	2680	0.11	as above
		0.043††	147	as above	3.14	<0.15?	2680	0.10	as above
Wolman and Brush [1961]		0.020††	9	···	0.67	0.26	···	0.05	straight, rectangular flume; plane bed; erodible banks; *Shimizu* [1989] sidewall correction‡‡
		0.024††	10	···	0.67	0.26	···	0.07	as above
		0.030††	12	···	0.67	0.26	···	0.07	as above
		0.024††	11	···	0.67	0.26	···	0.12	as above
		0.048††	86	···	2	0.5	···	0.16	as above
		0.049††	91	···	2	0.5	···	0.06	as above
		0.052††	94	···	2	0.5	···	0.12	as above
		0.036††	80	···	2	0.5	···	0.05	as above
		0.044††	86	···	2	0.5	···	0.09	as above
		0.030††	71	···	2	0.5	···	0.04	as above
Raudkivi [1963]§§		0.036††	6.0	···	0.40	0.42	2600	0.003	straight, rectangular flume; plane bed; *Vanoni and Brooks* [1957] sidewall correction‖,¶
Vanoni [1964]§§		0.097††	1.3	···	0.102	0.19	2650	0.0009	straight rectangular flume; plane bed; sidewall correction implicit; quartz grains
		0.126††	1.5	···	0.102	0.19	2650	0.001	as above
		0.120††	1.5	···	0.102	0.19	2650	0.001	as above

	0.226††	0.43	···	0.037	0.25	2490	0.0005	as above, but with glass beads
	0.228††	0.43	···	0.037	0.25	2490	0.0005	as above
Neill [1967]**	0.030††	328	···	6.2	~0.48?	2540	0.04	straight, rectangular flume; plane bed; *Shimizu* [1989] sidewall correction‡‡
	0.032††	340	···	6.2	~0.48?	2540	0.04	as above
	0.030††	327	···	6.2	~0.48?	2540	0.05	as above
	0.041††	382	···	6.2	~0.48?	2540	0.05	as above
	0.038††	372	···	6.2	~0.48?	2540	0.06	as above
	0.032††	339	···	6.2	~0.48?	2540	0.07	as above
	0.036††	359	···	6.2	~0.48?	2540	0.07	as above
	0.032††	337	···	6.2	~0.48?	2540	0.11	as above
	0.023††	289	···	6.2	~0.48?	2540	0.12	as above
	0.050††	675	···	8.5	~0.48?	2520	0.05	as above
	0.056††	713	···	8.5	~0.48?	2520	0.07	as above
	0.037††	584	···	8.5	~0.48?	2520	0.14	as above
	0.039	595	···	8.5	~0.48?	2520	0.28	as above
	0.037††	2099	···	20.0	~0.48?	2520	0.11	as above
	0.031††	1938	···	20.0	~0.48?	2520	0.14	as above
	0.036††	2066	···	20.0	~0.48?	2520	0.18	as above
	0.031	1935	···	20.0	~0.48?	2520	0.23	as above
	0.027	1802	···	20.0	~0.48?	2520	0.33	as above
	0.032	1950	···	20.0	~0.48?	2520	0.39	as above
	0.031	1928	···	20.0	~0.48?	2520	0.55	as above
	0.037††	259	···	5.0	0	2490	0.03	as above, but with glass grains
	0.039††	266	···	5.0	0	2490	0.04	as above
	0.042††	278	···	5.0	0	2490	0.04	as above
	0.038††	264	···	5.0	0	2490	0.04	as above
	0.037††	261	···	5.0	0	2490	0.05	as above
	0.027††	221	···	5.0	0	2490	0.08	as above
Rathburn and Guy [1967]	0.026	3.4	···	0.3	1.26	2650	0.005	straight, rectangular flume; plane bed *Vanoni and Brooks* [1957] sidewall correction ‖,¶
Ward [1968]‖‖	0.102	21	···	0.70	<0.5	2640	···	convergent-walled flume; plane bed; sidewall correction implicit; water fluid medium
	0.084	56	···	1.43	<0.5	2640	···	as above
	0.092	119	···	2.29	<0.5	2640	···	as above
	0.110	25	···	0.70	<0.5	3100	···	as above, but with taconite grains
	0.075	85	···	1.80	<0.5	3100	···	as above
	0.079	125	···	2.29	<0.5	3100	···	as above
	0.098	21	···	0.70	<0.5	2710	···	as above but with Douglas sand #2
	0.086	56	···	1.43	<0.5	2560	···	as above but with Douglas sand #1
	0.075	73	···	1.80	<0.5	2560	···	as above
	0.036	159	···	2.04	<0.5	11,340	···	as above, but with lead shot grains
	0.489	577	···	5.03	<0.5	7,830	···	as above, but with steel shot grains
	0.170	0.63	···	0.24	<0.5	2640	···	convergent-walled flume; plane bed; sidewall correction implicit; oil fluid medium; fully laminar flow
	0.103	2.4	···	0.70	<0.5	2640	···	as above
	0.063	11	···	2.29	<0.5	2640	···	as above
	0.066	7.8	···	1.80	<0.5	2640	···	as above
	0.148	1.2	···	0.37	<0.5	2950	···	as above, but with glass beads
	0.368	0.91	···	0.52	<0.5	1050	···	as above, but with styrene grains
	0.387	2.2	···	0.91	<0.5	1050	···	as above
	0.104	2.7	···	0.70	<0.5	3100	···	as above, but with taconite grains

Table 1b. (Continued)

Source	Note*	Laboratory Mixture Grain Size Distribution							
		$\tau^*_{c_{v50m}}$	Re^*_c†	Proposed τ^*_c Function Other Than Shields'	D_{50m}, mm	σ_{gm} (ϕ)	ρ_s, kg/m^3	D_{50m}/h_c‡	Experimental Conditions
		0.061	8.4	···	1.80	<0.5	3100	···	as above
		0.051	11	···	2.29	<0.5	3100	···	as above
		0.114	2.6	···	0.70	<0.5	2710	···	as above, but with Douglas sand #2
		0.065	7.9	···	1.80	<0.5	2710	···	as above
		0.081	6.1	···	1.43	<0.5	2560	···	as above, but with Douglas sand #1
		0.620	9.7	···	3.05	<0.5	930	···	as above, but with polyethylene grains
White [1970]		0.053††	36	···	2.2	~u	1050	<0.2	straight, rectangular flume; plane bed; sidewall correction; polystyrene grains
		0.037††	53	···	2	~u	1540	<0.2	as above, but with PVC grains
		0.055††	1.7	···	0.137	~u	2600	<0.2	as above, but with glass ballotini grains
		0.073††	0.94	···	0.088	~u	2600	<0.2	as above
		0.055††	2.2	···	0.17	~u	2520	<0.2	as above, but with natural grains
		0.058††	1.9	···	0.153	~u	2520	<0.2	as above
		0.071††	1.6	···	0.133	~u	2520	<0.2	as above
		0.066††	0.92	···	0.093	~u	2520	<0.2	as above
		0.073††	0.73	···	0.077	~u	2520	<0.2	as above
		0.125††	0.42	···	0.044	~u	2520	<0.2	as above
		0.102††	0.21	···	0.030	~u	2520	<0.2	as above
		0.103††	0.20	···	0.029	~u	2520	<0.2	as above
		0.146††	0.23	···	0.028	~u	2520	<0.2	as above
		0.110††	0.16	···	0.024	~u	2520	<0.2	as above
		0.112††	0.26	···	0.033	~u	2550	<0.2	as above, but with crushed silica grains
		0.151††	0.10	···	0.016	~u	2550	<0.2	as above
		0.037††	16	···	2.2	~u	1050	<0.2	as above, but with polystyrene grains in oil; fully laminar flow (?)
		0.034††	40	···	2	~u	1540	<0.2	as above, but with PVC grains
		0.143††	0.20	···	0.088	~u	2600	<0.2	as above, but with glass ballotini grains
		0.132††	0.32	···	0.133	~u	2520	<0.2	as above, but with natural grains
		0.122††	0.19	···	0.093	~u	2520	<0.2	as above
		0.166††	0.16	···	0.077	~u	2520	<0.2	as above
		0.218††	0.086	···	0.046	~u	2520	<0.2	as above
		0.254††	0.055	···	0.033	~u	2520	<0.2	as above
		0.288††	0.048	···	0.030	~u	2520	<0.2	as above
		0.219††	0.033	···	0.025	~u	2520	<0.2	as above
Grass [1970]‖‖	26	0.141†† (0.174)	0.87 (0.97)	···	0.090	<0.24	2650	<0.02?	straight, rectangular flume; plane bed; sidewall correction implicit
		0.131†† (0.154)	0.84 (0.91)	···	0.090	<0.24	2650	<0.02?	as above
		0.110†† (0.131)	1.6 (1.7)	···	0.115	<0.13	2650	<0.02?	as above
		0.086†† (0.095)	1.8 (1.9)	···	0.138	<0.13	2650	<0.03?	as above
		0.069†† (0.093)	2.1 (2.5)	···	0.165	<0.13	2650	<0.03?	as above
		0.072†† (0.079)	2.8 (2.9)	···	0.195	<0.11	2650	<0.04?	as above
		0.058 (0.091)	1.6 (2.0)	···	0.143	<0.74	2650	<0.03?	as above
Sternberg [1971]‖‖, ¶¶		0.094	5.9	···	0.42	1.09	···	$<2 \times 10^{-5}$	sandy, rippled, marine channel (Pickering Passage); form drag correction similar to that in note 3
		0.048	6.2	···	0.50	1.0	···	$<2 \times 10^{-5}$	as above
		0.038	5.5	···	0.50	1.0	···	$<2 \times 10^{-5}$	as above

		0.041	3.1	···	0.33	1.12	···	≪0.20	sandy marine channel (Clovis Passage) with random roughness elements; form drag correction similar to that in note 3
Everts [1973]‖‖		0.023††	145	···	3.57	<0.25?	2650	0.06	straight, rectangular flume; plane bed; *Williams* [1970] sidewall correction
		0.027††	157	···	3.57	<0.25?	2650	0.08	as above
		0.029††	162	···	3.57	<0.25?	2650	0.19	as above
		0.023††	51	···	1.79	<0.25?	2650	0.03	as above
		0.025††	54	···	1.79	<0.25?	2650	0.04	as above
		0.019††	47	···	1.79	<0.25?	2650	0.06	as above
		0.017††	44	···	1.79	<0.25?	2650	0.08	as above
		0.017††	16	···	0.895	<0.25?	2650	0.01	as above
		0.021††	17	···	0.895	<0.25?	2650	0.02	as above
		0.018††	16	···	0.895	<0.25?	2650	0.02	as above
		0.020††	17	···	0.895	<0.25?	2650	0.04	as above
		0.020††	7.2	···	0.508	<0.25?	2650	0.006	as above
		0.024††	8.0	···	0.508	<0.25?	2650	0.009	as above
		0.022††	7.7	···	0.508	<0.25?	2650	0.01	as above
		0.025††	8.1	···	0.508	<0.25?	2650	0.02	as above
		0.029††	5.2	···	0.359	<0.25?	2650	0.005	as above
		0.026††	4.9	···	0.359	<0.25?	3650	0.006	as above
		0.027††	5.1	···	0.359	<0.25?	2650	0.009	as above
		0.023††	4.6	···	0.359	<0.25?	2650	0.04	as above
		0.032††	3.3	···	0.254	<0.25?	2650	0.003	as above
		0.035††	3.4	···	0.254	<0.25?	2650	0.004	as above
		0.041††	3.7	···	0.254	<0.25?	2650	0.008	as above
		0.039††	2.1	···	0.18	<0.25?	2650	0.002	as above
		0.046††	2.3	···	0.18	<0.25?	2650	0.005	as above
		0.052††	1.5	···	0.127	<0.25?	2650	0.002	as above
		0.052††	1.5	···	0.127	<0.25?	2650	0.002	as above
		0.040††	1.3	···	0.127	<0.25?	2650	0.01	as above
		0.056††	3.9	···	0.18	<0.25?	4700	0.003	as above, but with ilmenite grains
		0.056††	3.9	···	0.18	<0.25?	4700	0.005	as above
		0.062††	4.1	···	0.18	<0.25?	4700	0.006	as above
		0.058††	2.3	···	0.127	<0.25?	4700	0.002	as above
		0.060††	2.4	···	0.127	<0.25?	4700	0.002	as above
		0.059††	2.4	···	0.127	<0.25?	4700	0.003	as above
		0.063††	2.4	···	0.127	<0.25?	4700	0.004	as above
		0.057††	1.4	···	0.09	<0.25?	4700	0.001	as above
		0.070††	1.5	···	0.09	<0.25?	4700	0.002	as above
		0.058††	1.4	···	0.09	<0.25?	4700	0.002	as above
		0.081††	1.6	···	0.09	<0.25?	4700	0.004	as above
Fernandez Luque and van Beek [1976]‖‖	28	0.039††	18	···	0.9	0.25	2640	0.01	straight, rectangular flume; plane bed; sidewall correction implicit; bed slope of 0°
		0.038††	48	···	1.8	0.25	2640	0.02	as above
		0.047††	127	···	3.3	0.25	2640	0.04	as above
		0.043††	74	···	1.8	0.25	4580	0.02	as above, but with magnetite grains
		0.039††	16	···	1.5	0.25	1340	0.01	as above, but with walnut (shell?) grains
		0.031	16	···	0.9	0.25	2640	0.01	straight, rectangular flume; plane bed; sidewall correction implicit; bed slope is 12°
		0.030	43	···	1.8	0.25	2640	0.02	as above
		0.037	114	···	3.3	0.25	2640	0.04	as above

Table 1b. (Continued)

Source	Note*	Laboratory Mixture Grain Size Distribution							
		$\tau^*_{c_{v50m}}$	Re^*_c†	Proposed τ^*_c Function Other Than Shields'	D_{50m}, mm	σ_{gm} (ϕ)	ρ_s, kg/m^3	D_{50m}/h_c‡	Experimental Conditions
		0.035	67	···	1.8	0.25	4580	0.02	as above, but with magnetite grains
		0.031	14	···	1.5	0.25	1340	0.01	as above, but with walnut (shell?) grains
		0.027	14	···	0.9	0.25	2640	0.01	straight, rectangular flume; plane bed; sidewall correction implicit; bed slope is 18°
		0.026	39	···	1.8	0.25	2640	0.02	as above
		0.031	112	···	3.3	0.25	2640	0.04	as above
		0.028	59	···	1.8	0.25	4580	0.02	as above, but with magnetite grains
		0.026	13	···	1.5	0.25	1340	0.01	as above, but with walnut (shell?) grains
		0.025	14	···	0.9	0.25	2640	0.01	straight, rectangular flume; plane bed; sidewall correction implicit; bed slope is 22°
		0.021	36	···	1.8	0.25	2640	0.02	as above
		0.027	99	···	3.3	0.25	2640	0.04	as above
		0.023	55	···	1.8	0.25	4580	0.02	as above, but with magnetite grains
		0.024	12	···	1.5	0.25	1340	0.01	as above, but with walnut (shell?) grains
From *Mantz* [1977]									
Schoklitsch [1914]**		0.066	176	···	3.06	0	2700	···	straight, rectangular flume; plane bed; slate grains; no sidewall correction (?)
		0.041	37	···	1.24	0	2700	···	as above
Ho [1939]**		0.018	265	···	6.71	0.56	2660	≤0.17	straight, rectangular flume; plane bed; slate grains; no sidewall correction (?)
		0.025††	225	···	5.71	0.46	2660	≤0.12	as above
		0.021	102	···	3.26	1.13	2700	≤0.09	as above
		0.034	65	···	2.21	0.90	2490	≤0.20	as above
		0.024	33	···	1.63	0.98	2450	≤0.05	as above
Mantz [1975]		0.094††	0.70	···	0.066	~0.20	2650	0.0007	straight, rectangular flume; plane bed; *Shimizu* [1989] sidewall correction;‡‡ quartz grains
		0.121††	0.79	···	0.066	~0.20	2650	0.0008	as above
		0.127††	0.81	···	0.066	~0.20	2650	0.001	as above
		0.122††	0.79	···	0.066	~0.20	2650	0.002	as above
		0.126††	0.81	···	0.066	~0.20	2650	0.003	as above
		0.155††	0.48	···	0.045	~0.20	2650	0.0004	as above
		0.147††	0.47	···	0.045	~0.20	2650	0.0006	as above
		0.134††	0.45	···	0.045	~0.20	2650	0.0008	as above
		0.127††	0.44	···	0.045	~0.20	2650	0.001	as above
		0.140††	0.46	···	0.045	~0.20	2650	0.002	as above
		0.140††	0.27	···	0.030	~0.20	2650	0.0003	as above
		0.133††	0.27	···	0.030	~0.20	2650	0.0004	as above
		0.164††	0.29	···	0.030	~0.20	2650	0.0005	as above
		0.161††	0.29	···	0.030	~0.20	2650	0.0008	as above
		0.165††	0.28	···	0.030	~0.20	2650	0.001	as above
		0.198††	0.12	···	0.015	~0.20	2650	0.0002	as above
		0.070††	0.77	···	0.076	~0.2?	2740	≤0.004	as above, but with micaceous flakes** and no sidewall correction
		0.062††	0.71	···	0.076	~0.2?	2740	≤0.004	as above

		0.055††	0.39	···	0.053	~0.2?	2740	≤0.003	as above
		0.070††	0.44	···	0.053	~0.2?	2740	≤0.003	as above
		0.061††	0.29	···	0.042	~0.2?	2740	≤0.002	as above
		0.068††	0.30	···	0.042	~0.2?	2740	≤0.002	as above
		0.063††	0.20	···	0.033	~0.2?	2740	≤0.002	as above
		0.076††	0.22	···	0.033	~0.2?	2740	≤0.002	as above
		0.092††	0.15	···	0.024	≥0.2?	2740	≤0.001	as above
		0.087††	0.15	···	0.024	~0.2?	2740	≤0.001	as above
		0.140††	0.10	···	0.016	~0.2?	2740	≤0.001	as above
Wimbush and Lesht [1979]‖‖‖, ¶¶	27	0.030	2.4	···	0.35	≤0.84	2930 (?)–1100	5×10^{-7}	sandy, rippled, marine channel (Straights of Florida); form drag correction similar to that in note 3
Yalin and Karahan [1979]		0.038††	25	···	1.00	<0.34–<0.54?	2650	0.16	straight, rectangular flume; plane bed; sidewall correction implicit?
		0.030††	9.4	···	0.56	<0.34–<0.54?	2650	0.12	as above
		0.113††	1.5	···	0.10	<0.34–<0.54?	2650	0.02	as above
		0.036††	6.1	···	0.40	<0.34–<0.54?	2650	0.09	as above
		0.053††	2.5	···	0.19	<0.34–<0.54?	2650	0.03	as above
		0.079††	1.8	···	0.14	0	2500	0.03	as above, but with glass bead grains
		0.178††	0.13	···	1.00	<0.34–<0.54	2650	0.09	as above, but with natural grains in a water-glycerin mixture and fully laminar flow
		0.156††	0.30	···	1.88	<0.34–<0.54	2650	0.24	as above
		0.135††	0.55	···	2.86	<0.34–<0.54	2650	0.38	as above
		0.172††	0.054	···	0.56	<0.34–<0.54	2650	0.04	as above
		0.110††	0.78	···	1.00	<0.34–<0.54	2650	0.10	as above
		0.092††	1.9	···	1.88	<0.34–<0.54	2650	0.30	as above
		0.141††	0.38	···	0.56	<0.34–<0.54	2650	0.04	as above
		0.086††	3.4	···	2.86	<0.34–<0.54	2650	0.41	as above
		0.091††	3.4	···	2.86	<0.34–<0.54	2650	0.25	as above
		0.134††	0.86	···	1.00	<0.34–<0.54	2650	0.07	as above
		0.143††	0.38	···	0.56	<0.34–<0.54	2650	0.03	as above
		0.110††	2.0	···	1.88	<0.34–<0.54	2650	0.16	as above
		0.140††	0.80	···	0.56	<0.34–<0.54	2650	0.04	as above
		0.069††	6.4	···	2.86	<0.34–<0.54	2650	0.31	as above
		0.086††	3.8	···	1.88	<0.34–<0.54	2650	0.18	as above
		0.106††	1.6	···	1.00	<0.34–<0.54	2650	0.09	as above
Ikeda [1982]		0.020††	8.7	···	0.42	0.36	···	0.006	laterally tilting wind tunnel; straight, rectangular walls; plane bed; *Adachi* [1962] sidewall correction
		0.047††	72	···	1.3	0.31	···	0.02	as above
Young and Mann [1985]¶¶	28	0.030	2.5	···	0.36	1.8	1500	1.5×10^{-5}	straight, rectangular sea flume; plane bed or low-amplitude bed forms; sidewall correction implicit; skeletal carbonate grains
		0.028	4.3	···	0.53	>2.1	1500	2.3×10^{-5}	as above
		0.109	1.6	···	0.18	<2.0	1500	1.4×10^{-5}	as above
		0.075	1.5	···	0.19	<2.1	1500	7.3×10^{-6}	as above
		0.026	0.58	···	0.14	<2.0	1500	5.3×10^{-6}	as above
		0.105	1.4	···	0.16	<2.1	1500	5.3×10^{-6}	as above
		0.059	2.0	···	0.25	<2.2	1500	1.0×10^{-5}	as above
		0.070	3.6	···	0.35	2.0	1500	1.5×10^{-5}	as above
		0.047	3.0	···	0.35	2.2	1500	2.3×10^{-5}	as above

Table 1b. (Continued)

Source	Note*	Laboratory Mixture Grain Size Distribution							
		$\tau^*_{c_{v50m}}$	Re^*_c†	Proposed τ^*_c Function Other Than Shields'	D_{50m}, mm	σ_{gm} (ϕ)	ρ_s, kg/m^3	D_{50m}/h_c‡	Experimental Conditions
Prager et al. [1996]¶¶		0.025††	7.1	···	0.5	≤0.5?	2660	0.04	straight, rectangular flume; plane bed; *Shimizu* [1989] sidewall correction;‡‡ well-rounded quartz grains
		0.021††	6.6	···	0.5	≤0.5?	2770	0.04	as above, but with ooid grains
		0.025††	7.3	···	0.5	≤0.5?	2730	0.04	as above, but with rounded, mixed carbonate and terrigenous grains
		0.022††	6.2	···	0.5	≤0.5?	2500	0.04	as above, but with platy, skeletal carbonate grains
		0.020	11	···	0.7	0.80	2700?	0.05	as above
		0.017	19	···	1.1	0.93	2670?	0.09	as above

Note that symbols for similar footnotes may be different in Tables 1a–1e. See notation section for symbols not previously defined in text. See respective appendix notes for values in parentheses. Here "u" denotes uniform grain sizes ($\sigma_g \leq 0.5$) and "m" denotes mixed grain sizes ($\sigma_g > 0.5$), where σ_g is the graphic standard deviation defined as $(\phi_{84} - \phi_{16})/2$ [*Folk*, 1974].

*See appendix.

†$Re^*_c = u^*_c D_{50}/\nu$. Where unreported by a source, Re^*_c values are back-calculated from available data (see footnote keyed to †, Table 1a).

‡Where unreported by a source, h_c values are back-calculated from critical depth-slope products using reported data (see footnote keyed to ‡, Table 1a).

§Here we describe grain protrusion in terms of projection and exposure [sensu *Kirchner et al.*, 1990].

‖Sidewall correction for the difference in wall and bed grain roughness but not for the proximity of walls (i.e., *W*/*h*).

¶Use of the average velocity in the *Einstein* [1942; 1950], *Johnson* [1942] and *Vanoni and Brooks* [1957] equations likely overestimates τ' (see note 3).

**Reported data are with respect to the mean nominal grain diameter. Nominal diameters are assumed equivalent to intermediate grain diameters [*Cui and Komar*, 1984]. Mean and median sizes are similar for near-uniform sediment.

††Used in Plate 1.

‡‡Sidewall correction applied by current authors. *Shimizu*'s [1989] correction accounts for both the difference in wall and bed grain roughness and the proximity of walls (i.e., *W*/*h*). We assumed a bed grain roughness 100 times greater than wall roughness for smooth flume walls.

§§Reported data are with respect to the geometric mean grain size.

‖‖Reported data are with respect to mean grain sizes. Mean and median grain sizes are assumed similar for near-uniform sediment.

¶¶Reported data are determined from bulk (i.e., surface and subsurface mixture) grain size sampling, treated here as mixture-based values.

Table 1c. Previously Reported $\tau^*_{c_{50}}$ Values: Competence (Largest Mobile Grain)

Source	Note*	Surface Grain-Size Distribution: $\tau^*_{c_{q50s}}$	Re^*_c†	Proposed τ^*_c Function Other Than Shields'	D_{50s}, mm	σ_{gs} (ϕ)	ρ_s, kg/m^3	D_{50s}/h_c‡	Experimental Conditions
Carling [1983]	29	0.020	6,629	$\tau^*_{c_{qi}} = 1.17Re_i^{*-0.46}$	62	~2	2710	0.29	natural, steep, gravel-bedded channel (Great Eggleshope Beck); coarse-grained plane bed/alternate bar morphology (?); no form drag or sidewall correction
		0.080	18,634	$\tau^*_{c_{qi}} = 4.99Re_i^{*-0.42}$	77	~1.7	2460	0.34	natural, steep, narrow, gravel-bedded channel (Carl Beck); coarse-grained plane bed morphology (?); no form drag or sidewall correction
Hammond et al. [1984]	30	0.025§	877	$\tau^*_{c_{qi}} = 0.025(D_i/D_{50s})^{-0.60}$	15.5	0.90	2650	≪0.20	natural, planar, tidal channel (West Solent)
Andrews and Erman [1986]	31	0.050§	8,377	$\tau^*_{c_{qi}} = 0.101(D_i/D_{50ss})^{-1.07}$	58	0.97	···	0.14	natural, meandering, pool-riffle channel (Sagehen Creek); no form drag or sidewall correction
From *Komar* [1987a]	32								
Milhous [1973]	33	0.027§	7,277	$\tau^*_{c_{qi}} = 0.044(D_i/D_{50ss})^{-0.43}$	63	<0.71	2850	0.20	same as first entry of Table 1a
Milhous [1973]	33	0.024	6,861	$\tau^*_{c_{qi}} = 0.044(D_i/D_{50ss})^{-0.53}$	63	<0.71	2850	0.23	as above
Carling [1983]	34	0.021	6,738	$\tau^*_{c_{qi}} = 0.045(D_i/D_{50})^{-0.68}$	62	~2	2710	0.28	same as *Carling* [1983], first entry of Table 1c (Great Eggleshope Beck)
Carling [1983]	34	0.022	6,896	$\tau^*_{c_{qi}} = 0.045(D_i/D_{50})^{-0.64}$	62	~2	2710	0.27	as above
Hammond et al. [1984]	35	0.027§	911	$\tau^*_{c_{qi}} = 0.045(D_i/D_{50})^{-0.71}$	15.5	0.90	2650	≪0.20	same as *Hammond et al.* [1984], second entry of Table 1c
From *Komar* [1987b]									
Fahnestock [1963]	36	0.031	21,033	···	134	1.79	···	0.61	natural, proglacial, braided channel (White River); no form drag or sidewall correction
Ferguson et al. [1989]		0.047§	37,880	$\tau^*_{c_{qi}} = 0.047(D_i/D_{50s})^{-0.88}$	73	···	2800	0.20	natural, proglacial, braided, gravel channel (White River); form drag and sidewall correction as in note 3
From *Komar and Carling* [1991]	37								
Milhous [1973]		0.028	7,601	$\tau^*_{c_{qi}} = 0.059(D_i/D_{50ss})^{-0.64}$	63	<0.71	2850	0.27	same as first entry of Table 1a
Komar and Carling [1991]		0.039§	9,182	$\tau^*_{c_{qi}} = 0.039(D_i/D_{50s})^{-0.82}$	62	~2	2710	0.15	same as *Carling* [1983] from *Komar* [1987a]
Ashworth et al. [1992]		0.049§	1,807	$\tau^*_{c_{qi}} = 0.049(D_i/D_{50s})^{-0.69}$	21	···	2650	0.07	same as *Ashworth et al.* [1992], sixth entry of Table 1a
Lepp et al. [1993]	38	0.149	28,421	$\tau^*_{c_{qi}} = 0.149(D_i/D_{50s})^{-0.40}$	91	0.40	···	0.35	Natural, steep, gravel-bedded river; bed form type not reported; *Shimizu* [1989] sidewall correction,‖ but no form drag correction
		0.143	24,693	$\tau^*_{c_{qi}} = 0.143(D_i/D_{50s})^{-0.50}$	84	0.33	···	0.45	as above
		0.155	40,645	$\tau^*_{c_{qi}} = 0.155(D_i/D_{50s})^{-0.47}$	114	0.38	···	0.48	as above

Table 1c. (Continued)

Source	Note*	Surface Grain Size Distribution							
		$\tau^*_{c_{q50s}}$	Re^*_c†	Proposed τ^*_c Function Other Than Shields'	D_{50s}, mm	σ_{gs} (ϕ)	ρ_s, kg/m^3	D_{50s}/h_c‡	Experimental Conditions
Ferguson [1994]		0.074	14,096	$\tau^*_{c_{qi}} = 0.074(D_i/D_{50s})^{-0.87}$	72	1.56	2650	0.38	natural boulder-bed stream (Roaring River); bed form type not reported; no sidewall correction; *Thompson and Campbell* [1979] form drag correction for relative roughness
		0.078	16,005	$\tau^*_{c_{qi}} = 0.078(D_i/D_{50s})^{-0.88}$	77	1.14	2650	0.40	as above
		0.061	34,701	$\tau^*_{c_{qi}} = 0.061(D_i/D_{50s})^{-0.89}$	140?	1.06?	2650	0.47?	as above
		0.070	24.606	$\tau^*_{c_{qi}} = 0.070(D_i/D_{50s})^{-0.78}$	106	1.06	2650	0.31	as above
		0.047§	11,943	$\tau^*_{c_{qi}} = 0.047(D_i/D_{50s})^{-0.69}$	75	···	2650	0.03	as above, but for the Gaula River
Wathen et al. [1995]		0.059§	2,025	$\tau^*_{c_{qi}} = 0.059(D_i/D_{50s})^{-0.70}$	21.3	~1.6	2650	0.02–0.21	same as *Wathen et al.* [1995], tenth entry of Table 1a

Source	Note*	Subsurface Grain Size Distribution							
		$\tau^*_{c_{q50ss}}$	Re^*_c†	Proposed τ^*_c Function Other Than Shields'	D_{50ss}, mm	σ_{gss} (ϕ)	ρ_s, kg/m^3	D_{50ss}/h_c‡	Experimental Conditions
Andrews and Erman [1986]		0.101	4,429	$\tau^*_{c_{qi}} = 0.101(D_i/D_{50ss})^{-1.07}$	30	2.25	···	0.07	same as *Andrews and Erman* [1986], third entry of Table 1c
From *Komar* [1987a]									
Milhous [1973]		0.044	1,662	$\tau^*_{c_{qi}} = 0.044(D_i/D_{50ss})^{-0.43}$	20	<2.67	2850	0.12	same as *Parker and Klingeman* [1982], first entry of Table 1a
Carling [1983]	39	0.037	2,570	$\tau^*_{c_{qi}} = 0.045(D_i/D_{50})^{-0.68}$	27	···	2710	0.16	same as *Carling* [1983], first entry of Table 1c
From *Komar and Carling* [1991]									
Milhous [1973]		0.059	1,974	$\tau^*_{c_{qi}} = 0.059(D_i/D_{50ss})^{-0.64}$	20	<2.67	2850	0.13	same as *Parker and Klingeman* [1982], first entry of Table 1a
Komar and Carling [1991]		0.077	3,707	$\tau^*_{c_{qi}} = 0.039(D_i/D_{50s})^{-0.82}$	27	···	2710	0.08	same as *Carling* [1983], first entry of Table 1c

Note that symbols for similar footnotes may be different in Tables 1a–1e. See notation section for symbols not previously defined in text.

*See appendix.

†$Re^*_c = u^*_c D_{50}/\nu$. Where unreported by a source, Re^*_c values are back-calculated from available data (see footnote keyed to †, Table 1a).

‡Where unreported by a source, h_c values are back-calculated from critical depth-slope products using reported data (see footnote keyed to ‡, Table 1a).

§Used in Plate 1.

‖Sidewall correction applied by current authors. *Shimizu*'s [1989] correction accounts for both the difference in wall and bed grain roughness and the proximity of walls (i.e., W/h). We assumed a bed grain roughness 100 times greater than wall roughness for smooth flume walls.

Table 1d. Previously Reported $\tau^*_{c_{50}}$ Values: Theoretical

		Surface Grain Size Distribution							
Source	Note*	$\tau^*_{c_{t50s}}$	Re^*_c†	Proposed τ^*_c Function Other Than Shields'	D_{50s}, mm	σ_{gs} (ϕ)	ρ_s, kg/m^3	D_{50s}/h_c‡	Experimental Conditions
White [1940]	40	0.209	44	see reference	0.9	~u	2600	na	theoretical plane bed; single grain within like bed; variable packing, projection and exposure;§ $\Phi = 45°$
		0.136	51	see reference	0.71	~u	7900	na	as above
		0.210	693	see reference	5.6	~u	2600	na	as above
		0.209	117	see reference	0.9	~u	2100	na	as above, but with air fluid medium
		0.208	1,829	see reference	5.6	~u	2100	na	as above
Chepil [1959]		0.018	···	see reference	···	u, m	···	na	theoretical plane bed undergoing en masse motion; variable packing, projection and exposure;§ $\Phi = 24°$
Egiazaroff [1965]‖		0.060	1,000	see reference	···	u, m	···	na	theoretical plane bed; single grain on like, uniform, or mixed-grain bed; significant projection and exposure§
Ikeda [1982]	41	0.061 (0.034)	1,000	see reference	···	0	···	na	theoretical plane bed; single grain on like, uniform bed; significant projection and exposure;§ $\Phi = 45°$
Naden [1987]	42	0.046 (0.030, 0.021)	>77 (62, 52)	see reference	>2	0	2650	na	theoretical plane bed; single grain on like, uniform bed; full projection and exposure;§ $\Phi = 35°$
		0.216 (0.124, 0.080)	>167 (127, 102)	see reference	>2	0	2650	na	as above, but with two grains on like, uniform bed; full projection, but no exposure§ for grain of interest
		0.063 (0.036, 0.023)	>90 (68, 55)	see reference	>2	0	2650	na	as above, but with single grain within like, uniform bed; no projection or exposure§
Wiberg and Smith [1987]		0.060	1,000	see reference	···	0	2650	na	theoretical plane bed; single grain on like, uniform bed; significant projection and exposure;§ $\Phi = 60°$
		0.040	1,000	see reference	···	0	2650	na	as above, but with $\Phi = 50°$
James [1990]		0.046	100	see reference	···	0	···	na	theoretical plane bed; single grain within bed; moderate projection and exposure;§ $\Phi = 64°$
		0.011	130	see reference	···	0?	···	na	theoretical plane bed; single grain on like, uniform bed; significant projection and exposure;§ $\Phi = 19°$
Kirchner et al. [1990]	43	0.125	325–480	see reference	3.74–4.85	~0.94–1.18	2650	na	theoretical plane bed; single grain on like, mixed-grain bed; distribution of friction angle, protrusion and exposure§
Buffington et al. [1992]	44	0.100	334–12,145	see reference	4.1–45	0.67–1.50	2650	na	theoretical plane bed; single grain on like, mixed-grain bed; distribution of friction angle, protrusion and exposure§
Bridge and Bennett [1992]		0.060	1,000	see reference	···	0	···	na	theoretical plane bed with $\Phi \approx 39°$, protrusion of 0.5 [sensu *Fenton and Abbott*, 1977], Corey shape factor of 1, and Powers roundness of 6 single grain on like, uniform bed

Table 1d. (Continued)

Source	Note*	Surface Grain Size Distribution: $\tau^*_{c_{t50s}}$	Re^*_c†	Proposed τ^*_c Function Other Than Shields'	D_{50s}, mm	σ_{gs} (ϕ)	ρ_s, kg/m^3	D_{50s}/h_c‡	Experimental Conditions
		0.042	10,000	see reference	...	0	...	na	as above
Jiang and Haff [1993]	45	0.086–0.161	700–1,000	see reference	7.2 (?)	m	2650	na	simulated, heterogeneous, plane bed surface undergoing a "slab" shear; variable projection and exposure§
Ling [1995]	46	0.050	500	see reference	...	0	...	na	theoretical plane bed; single grain on like, uniform bed; significant projection and exposure§

Note that symbols for similar footnotes may be different in Tables 1a–1e. See notation section for symbols not previously defined in text. See respective appendix notes for values in parentheses. Here "u" denotes uniform grain sizes ($\sigma_g \leq 0.5$), and "m" denotes mixed grain sizes ($\sigma_g > 0.5$), where σ_g is the graphic standard deviation defined as $(\phi_{84} - \phi_{16})/2$ [*Folk*, 1974]; na, not applicable.
*See appendix.
†$Re^*_c = u^*_c D_{50}/\nu$. Where unreported by a source, Re^*_c values are back-calculated from available data (see footnote keyed to †, Table 1a).
‡Where unreported by a source, h_c values are back-calculated from critical depth-slope products using reported data (see footnote keyed to ‡, Table 1a).
§Here we describe grain protrusion in terms of projection and exposure [sensu *Kirchner et al.*, 1990].
‖Reported data are with respect to mean grain sizes. Mean and median grain sizes are assumed similar for near-uniform sediment.

Table 1e. Previously Reported $\tau^*_{c_{50}}$ Values: Other

Source	Surface Grain Size Distribution: $\tau^*_{c_{50s}}$	Re^*_c†	Proposed τ^*_c Function Other Than Shields'	D_{50s}, mm	σ_{gs} (ϕ)	ρ_s, kg/m^3	D_{50s}/h_c‡	Experimental Conditions
			Equivalence of Bed Load and Surface Grain Size					
Çeçen and Bayazit [1973]	0.044	1,481	...	14.6	0.72	...	0.26	straight, rectangular flume; plane bed; no sidewall correction
From *Komar and Carling* [1991]								
Milhous [1973]	0.037	8,738	$\tau^*_{c_{q50l}} = 0.104(D_{50l}/D_{50ss})^{-0.89}$	63	<0.71	2850	0.20	same as *Parker and Klingeman* [1982], first entry of Table 1a
Komar and Carling [1991]	0.055	10,904	$\tau^*_{c_{q50l}} = 0.055(D_{50l}/D_{50s})^{-0.89}$	62	~2	2710	0.11	same as *Carling* [1983], first entry of Table 1c
			Smallest Transport Captured by Bed Load Trap					
Powell and Ashworth [1995]	0.010	2,790	...	49	...	2586	0.20	natural, straight, gravel-bedded channel with low-amplitude medial bar (River Wharfe); loose, open framework, subangular grains; no sidewall or form drag correction
	0.011	2,860	...	49	...	2586	0.18	as above
	0.055	6,700	...	49	...	2586	0.03	as above, but with imbricated algal-covered grains
	0.067	7,590	...	49	...	2586	0.03	as above

Note that symbols for similar footnotes may be different in Tables 1a–1e. See notation section for symbols not previously defined in text.
*See appendix.
†$Re^*_c = u^*_c D_{50}/\nu$. Where unreported by a source, Re^*_c values are back-calculated from available data (see footnote keyed to †, Table 1a).
‡Where unreported by a source, h_c values are back-calculated from critical depth-slope products using reported data (see footnote keyed to ‡, Table 1a).

Nikuradse [1933] sand grain roughness).

m mixed grain size.

n_g, n_b Manning roughnesses due to grains and the combined effects of grains and bed forms [*Meyer-Peter and Müller*, 1948].

Q, Q_b total volumetric fluid discharge and that acting on the grains and bed forms [*Meyer-Peter and Müller*, 1948].

Re_c^*, Re_{ci}^* critical grain/boundary Reynolds number for D_{50} and D_i.

u uniform grain size.

u^*, u_c^* general and critical shear velocities.

W/h width-to-depth ratio.

α coefficient.

β exponent.

θ angular bed surface slope.

ν kinematic viscosity.

ρ, ρ_s fluid and sediment densities.

σ_g, σ_{gs}, σ_{gss}, σ_{gm} sorting coefficient (*Folk*'s [1974] graphic standard deviation) and those for the surface, subsurface, and laboratory mixtures.

τ_0 total boundary shear stress.

τ', τ'', ... components of total boundary shear stress due to roughness elements such as grains (τ'), bed forms, walls, large woody debris, etc.

τ_c critical shear stress for incipient motion.

τ_c^* dimensionless critical shear stress for incipient motion.

$\tau_{c_i}^*$, $\tau_{c_{50}}^*$, $\tau_{c_{50s}}^*$, $\tau_{c_{50ss}}^*$, $\tau_{c_{50m}}^*$ τ_c^* of D_i, D_{50}, D_{50s}, D_{50ss}, and D_{50m}.

$\tau_{c_{qi}}^*$, $\tau_{c_{q50}}^*$, $\tau_{c_{q50s}}^*$, $\tau_{c_{q50ss}}^*$, $\tau_{c_{q50l}}^*$ τ_c^* of D_i, D_{50}, D_{50s}, D_{50ss}, and D_{50l} based on empirical competence equations determined from coupled bed load sampling and shear stress measurement.

$\tau_{c_{ri}}^*$, $\tau_{c_{r50}}^*$, $\tau_{c_{r50s}}^*$, $\tau_{c_{r50m}}^*$ τ_c^* of D_i, D_{50}, D_{50s}, and D_{50m} for a specified reference bed load transport rate.

$\tau_{c_{vi}}^*$, $\tau_{c_{v50}}^*$, $\tau_{c_{v50m}}^*$ τ_c^* of D_i, D_{50}, and D_{50m} based on visual observation of incipient motion.

ϕ_{16}, ϕ_{84} $\log_2$ grain sizes for which 16% and 84% of the grains are finer.

Φ intergranular friction angle.

Appendix: Notes for Tables 1a–1e

1. We estimated the exponent of the *Parker and Klingeman* [1982] $\tau_{c_{ri}}^*$ function from their Figure 3. To calculate D_{50s}/h_c, we used a slope of 0.01 based on armor-breaching discharges (over 40 feet^3/s (1.13 m^3/s)) during the winter of 1971 [*Milhous*, 1973, Table I-3]; except where reported differently, we assumed this same slope for all sources using *Milhous*' [1973] data.

2. We calculated $\tau_{c_{r50s}}^*$ with $D_i = D_{50s} = 54$ mm [*Parker and Klingeman*, 1982] and $D_{50ss} = 19.5$ mm [*Wilcock and Southard*, 1988, Table 1].

3. D_{50s} values are averages of those reported in *Ashworth and Ferguson*'s [1989] Table 1. Although *Ashworth and Ferguson* [1989] used local velocity profiles rather than depth-slope products to determine shear stress, they used the full velocity profile rather than just near-bed values. The full profile includes all local roughness effects (bed form drag, etc.) and likely overestimates the effective shear stress (τ') (see discussion of segmented velocity profiles by *Middleton and Southard* [1984] and *Smith and McLean* [1977]). Their local velocity measures do, however, implicitly account for sidewall effects.

4. We estimated $\tau_{c_{r50s}}^*$ from *Wilcock and Southard*'s [1988] Oak Creek equation using the same D_i and D_{50ss} values as those in note 2 but with the coefficient of the equation reduced by 55% for bed form drag [*Wilcock*, 1993].

5. We calculated $\tau_{c_{r50s}}^*$ from the Shields equation using $\tau_{c_{r50s}}$ determined from *Wilcock and McArdell*'s [1993] Figure 8 expression, with D_{50s} estimated by averaging their Figure 5 data for runs 7b, 7c, 2, 4, 5, 6, and 14c (assumed to be equal to "start-up").

6. We estimated $\tau_{c_{r50s}}^*$ for runs 4 and 5 from *Day*'s [1981] Figure 2 using D_{50s} values [*Day*, 1981, Figure 1] from the immediately preceding runs (i.e., 3 and 4, respectively) and recognizing that τ_c^* is the square of the Ackers-White mobility number.

7. We calculated $\tau_{c_{r50s}}^*$ from the Shields equation using $\tau_{c_{r50s}}$ regressed from particle velocity and u^* data for D_{50s} values in *Meland and Norrman*'s [1966] Figure 4.

8. We estimated $\tau_{c_{r50m}}^*$ and Re_c^* values from *Shields*' [1936] Figure 6. Because the corresponding grain sizes are unreported by Shields, we assigned D_{50m} values reported by each source based on a sensible match of grain size with estimated $\tau_{c_{r50m}}^*$ and Re_c^* pairs. Kramer's data are included here, however, it is uncertain if they are reference- or visual-based values; Kramer measured bed load transport rates but did not report them. D_{50m} and h_c values for *Casey* [1935] are from *Tison* [1953].

9. Using data in *Johnson*'s [1943] Tables 27–30, we linearly extrapolated τ_c values from plots of bed load transport rate versus shear stress for each sediment mixture and used these data to calculate $\tau_{c_{r50m}}^*$ values from the Shields equation. Lack of bedload size distributions precluded analysis of nonlinear relationships between bedload transport and shear stress using a *Parker and Klingeman* [1982] type method.

10. Curiously, *Gilbert*'s [1914] data analyzed in this fashion are very different than the other reference-based data and are excluded from our analysis.

11. We applied the method of note 7 to *Meland and Norrman*'s [1969] Figure 5, with $D_{50m} \approx 3.9$ mm [*Meland and Norrman*, 1969].

12. Although *Paintal* [1971] questions the existence of a definitive threshold for mobility [see also *Lavelle and Mofjeld*,

1987], two potential $\tau^*_{c_{r50m}}$ values can be estimated from his analysis. Extrapolating high bed load transport rates to a zero value yields $\tau^*_{c_{r50m}} \approx 0.05$ for D_{50m} values of 2.5 and 7.95 mm [*Paintal*, 1971, Figure 8]. The resultant $\tau^*_{c_{50}}$ and Re^*_c pairs agree with other referenced-based values determined by unreported curve-fitting techniques [e.g., *Shields*, 1936]. However, a more appropriate nonlinear fit of *Paintal*'s [1971, Figure 8] data can yield $\tau^*_{c_{50}}$ values as low as 0.01, depending on the chosen reference bedload transport rate.

13. We corrected *Mizuyama*'s [1977] modified Shields equation for a neglected buoyancy term (left-hand side of his equation (3.27); see work by *Wiberg and Smith* [1987] for a similar correct derivation). Using this corrected equation, we calculated $\tau^*_{c_{r50m}}$ values with data from *Mizuyama*'s [1977] Tables 3.1 and 3.2; $\tau^*_{c_{r50m}}$ values using a traditional Shields equation are shown in parentheses for comparison. Φ values used by *Mizuyama* [1977] are mass angles of repose for the bulk sediment mixture [sensu *Miller and Byrne*, 1966], rather than intergranular values.

14. The $\tau^*_{c_{r50m}}$ is for the lowest dimensionless bed load transport rate (10^{-6}) of the composite data set [*Pazis and Graf*, 1977, Figure 3].

15. We calculated $\tau^*_{c_{r50m}}$ values using *Bathurst et al.*'s [1987] equation (15.1) and values in their Table 15.3; equivalent $\tau^*_{c_{r50m}}$ values determined from a traditional Shields expression are shown in parentheses for comparison. We estimated Re^*_c values from *Bathurst et al.*'s [1987] Figure 15.3. As with *Mizuyama* [1977], Φ is the mass angle of repose of the sediment mixture.

16. We estimated $\tau^*_{c_{r50m}}$ values from *Bathurst et al.*'s [1987] Figure 15.3. Equivalent $\tau^*_{c_{r50m}}$ values using a traditional Shields expression are shown in parentheses [*Bathurst et al.*, 1979, Table 6].

17. We calculated $\tau^*_{c_{r50m}}$ from the Shields equation using $\tau_{c_{r50m}}$ of *Li and Komar*'s [1992] Figure 1b.

18. Using *Day*'s [1980] Figure 9 we determined $\tau^*_{c_{r50m}}$ values for dimensionless particle sizes corresponding to reported D_{50m} values [*Day*, 1980, Table 1], recognizing that τ^*_c is the square of the Ackers-White mobility number.

19. We estimated $\tau^*_{c_{r50m}}$ for run 3 from *Day*'s [1981] Figure 2 using D_{50m} of *Day*'s [1981] Figure 1 and recognizing that τ^*_c is the square of the Ackers-White mobility number.

20. We calculated $\tau^*_{c_{r50m}}$ from the *Parker and Klingeman* [1982] method as modified by *Ashworth and Ferguson* [1989] using data reported in *Leopold and Emmett*'s [1976, 1977] Tables 1 and 2.

21. Using the Shields equation we developed power law functions for $\tau^*_{c_n}$ from data in *Wilcock*'s [1992a] Figure 6.5 and Table 6.2.

22. We used the same procedure as in note 5, but with $D_t = D_{50m}$ estimated from the bulk bed distribution of *Wilcock and McArdell*'s [1993] Figure 5.

23. *Coleman* [1967] reports critical boundary Reynolds numbers in terms of u (the flow velocity measured at a height of $0.5D_{50s}$) rather than u^*. Consequently, his Re_c values must be converted to Re^*_c values by replacing u with u^*. We used Re^*_c values estimated from *Coleman*'s [1967] data by *Fenton and Abbott* [1977], but we did not use their corrected $\tau^*_{c_{50}}$ values, as *Coleman*'s [1967] shear stresses are not calculated from measures of u but instead are based on direct measures of strain and can be read from his Figure 3 without need for conversion. *Fenton and Abbott*'s [1977] $\tau^*_{c_{50}}$ values are shown for comparison in parentheses.

24. Reported data were derived from *Gilbert*'s [1914] Table 10 using his definition of incipient motion (i.e., "several grains moving" from a plane-bed surface [*Gilbert*, 1914, pp. 68, 71]) which we consider similar to *Kramer*'s [1935] "medium movement."

25. We calculated the first two $\tau^*_{c_{v50m}}$ and Re^*_c pairs from *White*'s [1940] Table 1 (experiments 1a, 1bii, and 2a) assuming $\rho_s = 2650$ kg/m^3 and $\rho \approx 900$ kg/m^3; ρ was estimated by comparing the reported depth-slope products [*White*, 1940, Table 1, "from d"] with those calculated for a fluid medium of water. We calculated the third $\tau^*_{c_{v50m}}$ and Re^*_c pair from *White*'s [1940, p. 328] data assuming $\nu = 10^{-6}$ m^2/s. All other reported values were taken from *White*'s [1940] Table 2.

26. Reported data are derived from *Grass*' [1970] averages of instantaneous shear stresses and are assumed equivalent to time-averaged values; instantaneous equivalents are shown in parentheses for comparison. *Grass*' [1970] direct shear stress measures implicitly account for sidewall effects.

27. We calculated $\tau^*_{c_{v50m}}$ from the Shields equation using the reported u^*_c value for initiation of grain motion [*Wimbush and Lesht*, 1979, Table 1], $\rho = 1027.6$ kg/m^3 (sea water of 3.5% salinity and 7.3°C [*Todd*, 1964]) and $\rho_s = 2015$ kg/m^3. We estimated ρ_s by averaging the densest possible carbonate (aragonite) with the least dense skeletal test measured by *Wimbush and Lesht* [1979].

28. We estimated $\tau^*_{c_{v50m}}$ by replacing the mean sand diameter in reported Shields stresses with D_{50m} values determined from the full grain size data of *Young and Mann*'s [1985] Table 1. We calculated corresponding Re^*_c values in a similar fashion.

29. The $\tau^*_{c_{q50s}}$ of Great Eggleshope Beck was calculated from the Shields equation, with D_{50s} taken as the median grain size of the framework distribution [*Komar and Carling*, 1991, Table 1] and $\tau_{c_{q50s}}$ determined from *Carling*'s [1983] equation (7) using the above D_{50s} value. The framework distribution is observationally similar to the censored (i.e., armored) surface layer distribution [*Carling and Reader*, 1982]; $\tau^*_{c_{q50s}}$ for Carl Beck was calculated in a similar fashion using a median framework gravel size estimated from *Carling*'s [1989] Figure 2, with the distribution truncated at 4 mm [*Carling*, 1989].

30. We developed a power law function for $\tau^*_{c_{qi}}$ using D_i and $\tau^*_{c_{qi}}$ data from *Hammond et al.*'s [1984] Table 1 and $D_{50s} = 15.5$ mm estimated from the grab sample data of their Figure 3 truncated at 2 mm; the surface material was observationally devoid of sand [*Hammond et al.*, 1984].

31. Rather than using the *Andrew*'s [1983] equation, we regressed a power law function through *Andrews and Erman*'s [1986] Figure 7 data and evaluated $\tau^*_{c_{q50s}}$ with $D_i = D_{50s} = 58$ mm and $D_{50ss} = 30$ mm [*Andrews and Erman*, 1986].

32. Using bed load transport data from *Milhous* [1973], *Carling* [1983], and *Hammond et al.* [1984], *Komar* [1987a] developed empirical competence equations for each study site, expressing competence as a power law function between shear stress and the largest mobile grain size [*Komar*, 1987a, Table 1]. To facilitate convergence of different data sets, *Komar* [1987a] proposed that Shields stress be expressed as a power law function of the form $\tau^*_{c_{qi}} = \alpha(D_i/D_{50})^\beta$ (similar to that used by *Parker et al.* [1982] and *Andrews* [1983]), where D_{50} is a generic term that *Komar* [1987a] inconsistently evaluated as either D_{50ss} or the "crossover" grain size [*Komar*, 1987a, p. 205]. For *Milhous*' [1973] data, *Komar* [1987a] set $D_{50} = D_{50ss}$ and algebraically manipulated the competence equation into the desired form of $\tau^*_{c_{qi}}$ [*Komar*, 1987a, p. 207]. For the *Carling* [1983] and *Hammond et al.* [1984] data, *Komar* [1987a] chose D_{50} values based on the empiricism that competence curves

cross the *Miller et al.* [1977] incipient motion curve at values of $D_i \approx D_{50}$, as demonstrated by *Day*'s [1980] data [*Komar*, 1987a, Figure 2], where $D_{50} = D_{50m}$ for *Day*'s [1980] data. However, the crossover value for *Carling*'s [1983] data (20 mm [*Komar*, 1987a, Figure 3]) is similar to the D_{50ss} value for that site (27 mm [*Komar and Carling*, 1991, Table 1]); while the *Hammond et al.* [1984] D_{50ss} value is not known, the crossover value (7.5 mm [*Komar*, 1987a, Table 1]) is less than D_{50s} (15.5 mm, note 30) and more like the D_{50} of their grab sample (10.3 mm [*Hammond et al.*, 1984, Figure 3]) which is likely to be composed predominantly of subsurface material. These observations indicate that *Komar*'s [1987a] $\tau^*_{c_{qi}}$ equations for *Milhous* [1973], *Carling* [1983], and *Hammond et al.* [1984] [*Komar*, 1987a, Table 1] are functions of median grain sizes similar or equal to those of the subsurface (i.e., *Komar*'s [1987a] generic D_{50} is defined as D_{50ss} in the Milhous equation and is roughly equivalent to D_{50ss} in the Carling and Hammond et al. equations).

Komar [1987a, Figure 4] fixed α values for the *Carling* [1983] and *Hammond et al.* [1984] $\tau^*_{c_{qi}}$ equations from crossover points with the *Miller et al.* [1977] curve, forcing $\alpha = 0.045$ and leaving β to be back-calculated. *Komar* [1987a] found that the resultant $\tau^*_{c_{qi}}$ equation for *Carling*'s [1983] data appeared to describe *Milhous*' [1973] data quite well, so he used it to represent *Milhous*' [1973] data, abandoning the algebraically defined Milhous equation (cf. p. 207, Figure 5, and Table 1 of *Komar* [1987a]). Rejecting this unsound rationale, we have maintained the original algebraically defined Milhous equation in Table 1c (as also preferred by *Komar and Shih* [1992]).

We calculated $\tau^*_{c_{q50s}}$ values from these "derived" $\tau^*_{c_{qi}}$ equations using values of $D_i = D_{50s}$ culled from other sources (see following notes) and D_{50} as defined by *Komar* [1987a, Table 1]. *Komar*'s [1987a] $\tau^*_{c_{qi}}$ equations for *Day*'s [1980] data were not used, as they represent $D_i/D_{50m} > 1$ only [*Komar*, 1987a, p. 209].

33. We calculated $\tau^*_{c_{q50s}}$ from the algebraically manipulated Milhous equation [*Komar*, 1987a, p. 207] and values of $D_{50} = D_{50ss} = 20$ mm [*Komar*, 1987a, Table 1] and $D_i = D_{50s} = 63$ mm [*Milhous*, 1973, Table 2; *Winter*, 1971]. We estimated a second set of values from a power law fit of data presented in *Komar*'s [1987a] Figure 5.

34. We calculated $\tau^*_{c_{q50s}}$ from the Carling equation [*Komar*, 1987a, Table 1] and values of $D_{50} \approx 20$ mm [*Komar*, 1987a, Table 1] and $D_i = D_{50s} = 62$ mm, the median grain size of the framework distribution [*Komar and Carling*, 1991, Table 1] (see also note 29). We estimated a second set of values from a power law fit of data presented in *Komar*'s [1987a] Figure 6.

35. We calculated $\tau^*_{c_{q50s}}$ from the *Hammond et al.* [1984] $\tau^*_{c_{qi}}$ equation [*Komar*, 1987a, Table 1] and values of $D_{50} = 7.5$ mm [*Komar*, 1987a, Table 1] and $D_i = D_{50s} = 15.5$ mm (note 30).

36. We calculated $\tau_{c_{q50s}}$ from the Fahnestock competence equation reported by *Komar* [1987b, Table 1], and used this value to determine $\tau^*_{c_{q50s}}$ from the Shields equation. For these calculations D_{50s} was determined from the composite White River grain size data [*Fahnestock*, 1963, Table 2].

37. We calculated $\tau^*_{c_{q50s}}$ values from relevant equations [*Komar and Carling*, 1991, Figure 9] and grain sizes [*Milhous*, 1973, p. 16; *Komar and Carling*, 1991, Table 1]. Although the legend for *Komar and Carling*'s [1991] Figure 9 indicates that the Carling equation is expressed as a function of D_{50ss}, the normalizing grain size used by the authors (62 mm) is that of the framework gravel [*Komar and Carling*, 1991, p. 498], which is equivalent to the censored (i.e., armored) surface size [*Carling and Reader*, 1982].

38. Values of $\tau^*_{c_{q50s}}$ were determined from power functions for $\tau^*_{c_{qi}}$ developed from *Lepp et al.*'s [1993, Tables 2–4] data.

39. We used $D_i = D_{50ss} = 27$ mm [*Komar and Carling*, 1991, Table 3] and $D_{50} = 20$ mm (see note 32).

40. We determined $\tau^*_{c_{t50s}}$ values using the Shields equation and $\tau_{c_{t50s}}$ values presented in *White*'s [1940] Table 2. However, he erroneously adds $\tan\theta$ to $\tan\Phi$, rather than subtracting it [cf. *Wiberg and Smith*, 1987]; our reported values reflect this correction.

41. The $\tau^*_{c_{t50s}}$ values were estimated from *Ikeda*'s [1982] Figure 5 for dimensionless lift-to-drag ratios of 0 and 0.8 (shown in parentheses).

42. Reported $\tau^*_{c_{t50s}}$ values are means for velocity fluctuations of zero, one, and two standard deviations, respectively [*Naden*, 1987, Table 2].

43. Φ and grain protrusion measurements were made from flume-worked heterogeneous bed surfaces with plane-bed or low-amplitude topography. The specific $\tau^*_{c_{t50s}}$ value reported here was read from *Kirchner et al.*'s [1990] Figure 18 for $D/K_{50} = 1$ and $n = 10$.

44. Φ measurements were made from bed surfaces of a natural pool-riffle stream (Wildcat Creek), and protrusion values were derived from *Kirchner et al.*'s [1990] experiments. The specific $\tau^*_{c_{t50s}}$ value reported here was read from *Buffington et al.*'s [1992] Figure 13 for $D/K_{50} = 1$ and $n = 0.1$.

45. Reported $\tau^*_{c_{t50s}}$ values bracket the calculated threshold of "continuous" motion, defined as one or more particles moving at all times during a simulation [*Jiang and Haff*, 1993].

46. *Ling* [1995] proposes two Shields curves representing sediment motion characterized by lifting and rolling, respectively. These curves coalesce at high Re^*_c values. The $\tau^*_{c_{t50s}}$ value reported here is half that of *Ling*'s [1995] Figure 3, corresponding to $k_s/D_{50s} = 1$ [*Ling*, 1995, p. 477].

Acknowledgments. This work was funded by the Pacific Northwest Research Station of the U.S. Department of Agriculture Forest Service (cooperative agreement PNW 94-0617) and by the Washington State Timber, Fish, and Wildlife agreement (TFW-SH10-FY93-004, FY95-156). Bill Dietrich, Peter Wilcock, and two anonymous reviewers provided insightful criticism that significantly improved this work.

References

Ackers, P., and W. R. White, Sediment transport: New approach and analysis, *J. Hydraul. Div. Am. Soc. Civ. Eng.*, *99*, 2041–2060, 1973.

Adachi, S., The effects of side walls in rectangular cross sectional channel, *Proc. Jpn. Soc. Civ. Eng.*, *81*, 17–26, 1962.

Aksoy, S., The influence of the relative depth on threshold of grain motion, in *Proceedings of the International Association for Hydraulic Research International Symposium on River Mechanics*, pp. 359–370, Int. Assoc. for Hydraul. Res., Delft, Netherlands, 1973.

Andrews, E. D., Entrainment of gravel from naturally sorted riverbed material, *Geol. Soc. Am. Bull.*, *94*, 1225–1231, 1983.

Andrews, E. D., Marginal bed load transport in a gravel-bed stream, Sagehen Creek, California, *Water Resour. Res.*, *30*(7), 2241–2250, 1994.

Andrews, E. D., and D. C. Erman, Persistence in the size distribution of surficial bed material during an extreme snowmelt flood, *Water Resour. Res.*, *22*, 191–197, 1986.

Andrews, E. D., and J. M. Nankervis, Effective discharge and the design of channel maintenance flows for gravel-bed rivers, in *Natural and Anthropogenic Influences in Fluvial Geomorphology, Geophys. Monogr. Serv.*, vol. 89, edited by J. E. Costa, A. J. Miller, K. W. Potter, and P. R. Wilcock, pp. 151–164, AGU, Washington, D. C., 1995.

Ashida, K., and M. Bayazit, Initiation of motion and roughness of flows in steep channels, in *Proceedings of the 15th Congress of the International Association for Hydraulic Research*, vol. 1, pp. 475–484, Int. Assoc. for Hydraul. Res., Delft, Netherlands, 1973.

Ashworth, P. J., and R. I. Ferguson, Size-selective entrainment of bed load in gravel bed streams, *Water Resour. Res.*, *25*, 627–634, 1989.

Ashworth, P. J., R. I. Ferguson, P. E. Ashmore, C. Paola, D. M. Powell, and K. L. Prestegaard, Measurements in a braided river chute and lobe, 2, Sorting of bed load during entrainment, transport, and deposition, *Water Resour. Res.*, *28*, 1887–1896, 1992.

Bathurst, J. C., R. M. Li, and D. B. Simons, Hydraulics of mountain rivers, *Rep. CER78-79JCB-RML-DBS55*, 229 pp., Eng. Res. Cent., Colo. State Univ., Fort Collins, 1979.

Bathurst, J. C., W. H. Graf, and H. H. Cao, Initiation of sediment transport in steep channels with coarse bed material, in *Mechanics of Sediment Transport*, edited by B. M. Sumer and A. Müller, pp. 207–213, A. A. Balkema, Rotterdam, 1983.

Bathurst, J. C., W. H. Graf, and H. H. Cao, Bed load discharge equations for steep mountain rivers, in *Sediment Transport in Gravel-bed Rivers*, edited by C. R. Thorne, J. C. Bathurst, and R. D. Hey, pp. 453–491, John Wiley, New York, 1987.

Bray, D. I., Evaluation of effective boundary roughness for gravel-bed rivers, *Can. J. Civ. Eng.*, *7*, 392–397, 1980.

Bridge, J. S., and S. J. Bennett, A model for the entrainment and transport of sediment grains of mixed sizes, shapes, and densities, *Water Resour. Res.*, *28*, 337–363, 1992.

Bridge, J. S., and D. F. Dominic, Bed load grain velocities and sediment transport rates, *Water Resour. Res.*, *20*, 476–490, 1984.

Brooks, N. H., Mechanics of streams with movable beds of fine sand, *Trans. Am. Soc. Civ. Eng.*, *123*, 526–549, 1958.

Brownlie, W. R., Flow depth in sand-bed channels, *J. Hydraul. Eng.*, *109*, 959–990, 1983.

Buffington, J. M., Effects of hydraulic roughness and sediment supply on surface textures of gravel-bedded rivers, M.S. thesis, 184 pp., Univ. of Wash., Seattle, 1995.

Buffington, J. M., W. E. Dietrich, and J. W. Kirchner, Friction angle measurements on a naturally formed gravel streambed: Implications for critical boundary shear stress, *Water Resour. Res.*, *28*, 411–425, 1992.

Carling, P. A., Threshold of coarse sediment transport in broad and narrow natural streams, *Earth Surf. Processes Landforms*, *8*, 1–18, 1983.

Carling, P. A., Bedload transport in two gravel-bedded streams, *Earth Surf. Processes Landforms*, *14*, 27–39, 1989.

Carling, P. A., and N. A. Reader, Structure, composition and bulk properties of upland stream gravels, *Earth Surf. Processes Landforms*, *7*, 349–365, 1982.

Carling, P. A., A. Kelsey, and M. S. Glaister, Effect of bed roughness, particle shape and orientation on initial motion criteria, in *Dynamics of Gravel-bed Rivers*, edited by P. Billi, R. D. Hey, C. R. Thorne, and P. Tacconi, pp. 24–39, John Wiley, New York, 1992.

Carson, M. A., and G. A. Griffiths, Tractive stress and the onset of bed particle movement in gravel stream channels: Different equations for different purposes, *J. Hydrol.*, *79*, 375–388, 1985.

Casey, H., Über geschiebebewegung, *Mitt. Preuss. Versuchsanst. Wasserbau Schiffbau*, *19*, 86, 1935.

Çeçen, K., and M. Bayazit, Critical shear stress of armored beds, in *Proceedings of the 15th Congress of the International Association for Hydraulic Research*, vol. 1, pp. 493–500, Int. Assoc. for Hydraul. Res., Delft, Netherlands, 1973.

Chang, Y. L., Laboratory investigation of flume traction and transportation, *Trans. Am. Soc. Civ. Eng.*, *104*, 1246–1284, 1939.

Cheng, E. D. H., Incipient motion of large roughness elements in turbulent open channel flow, Ph.D. dissertation, 179 pp., Utah State Univ., Logan, 1970.

Chepil, W. S., Equilibrium of soil grains at the threshold of movement by wind, *Soil Sci. Soc. Proc.*, *23*, 422–428, 1959.

Church, M., Palaeohydrological reconstructions from a Holocene valley fill, in *Fluvial Sedimentology*, *Can. Soc. Petrol. Geol. Mem.*, vol. 5, edited by A. D. Miall, pp. 743–772, Can. Soc. of Petrol. Geol., Calgary, Alberta, Canada, 1978.

Chyn, S. D., An experimental study of the sand transporting capacity of flowing water on a sandy bed and the effect of the composition of the sand, M.S. thesis, 33 pp., Mass. Inst. of Technol., Cambridge, 1935.

Clifford, N. J., A. Robert, and K. S. Richards, Estimation of flow resistance in gravel-bedded rivers: A physical explanation of the multiplier of roughness length, *Earth Surf. Processes Landforms*, *17*, 111–126, 1992.

Coleman, N. L., A theoretical and experimental study of drag and lift forces acting on a sphere resting on a hypothetical streambed, in *Proceedings of the 12th Congress of the International Association for Hydraulic Research*, vol. 3, pp. 185–192, Int. Assoc. Hydraul. Res., Delft, Netherlands, 1967.

Cui, B., and P. D. Komar, Size measures and the ellipsoidal form of clastic sediment particles, *J. Sediment. Petrol.*, *54*, 783–797, 1984.

Day, T. J., A study of the transport of graded sediments, *Rep. IT190*, 10 pp., Hydraul. Res. Stn., Wallingford, U. K., 1980.

Day, T. J., An experimental study of armouring and hydraulic properties of coarse bed material channels, in *Erosion and Sediment Transport in Pacific Rim Steeplands*, *Publ. 132*, edited by T. R. H. Davies and A. J. Pearce, pp. 236–251, Int. Assoc. of Hydrol. Sci., Gentbrugge, Belgium, 1981.

Dhamotharan, S., A. Wood, G. Parker, and H. Stefan, Bedload transport in a model gravel stream, *Proj. Rep. 190*, St. Anthony Falls Hydraul. Lab., Univ. of Minn., Minneapolis, 1980.

Dietrich, W. E., J. D. Smith, and T. Dunne, Boundary shear stress, sediment transport and bed morphology in a sand-bedded river meander during high and low flow, in *River Meandering, Proceedings of the Conference Rivers '83*, edited by C. M. Elliot, pp. 632–639, Am. Soc. Civ. Eng., New York, 1984.

Dietrich, W. E., J. W. Kirchner, H. Ikeda, and F. Iseya, Sediment supply and the development of the coarse surface layer in gravel-bedded rivers, *Nature*, *340*, 215–217, 1989.

Diplas, P., Bedload transport in gravel-bed streams, *J. Hydraul. Eng.*, *113*, 277–292, 1987.

Diplas, P., and J. B. Fripp, Properties of various sediment sampling procedures, *J. Hydraul. Eng.*, *118*, 955–970, 1992.

Diplas, P., and A. J. Sutherland, Sampling techniques for gravel sized sediments, *J. Hydraul. Eng.*, *114*, 484–501, 1988.

Egiazaroff, I. V., Calculation of nonuniform sediment concentrations, *J. Hydraul. Div. Am. Soc. Civ. Eng.*, *91*, 225–247, 1965.

Einstein, H. A., Formulas for the transportation of bed load, *Trans. Am. Soc. Civ. Eng.*, *107*, 561–597, 1942.

Einstein, H. A., The bed-load function for sediment transportation in open channel flows, *U.S. Dep. Agric. Soil Conserv. Serv. Tech. Bull. 1026*, 73 pp., 1950.

Einstein, H. A., and Barbarossa, N. L., River channel roughness, *Trans. Am. Soc. Civ. Eng.*, *117*, 1121–1146, 1952.

Engels, H., Grossmodellversuche über das Verhalten eines geschiebeführenden gewundenen Wasserlaufes unter der Einwirkung sechselnder Wasserstande und verschiedenartiger Eindeichungen, *Wasserkraft Wasserwirt.*, no. 3/4, 1932.

Engels, H., and H. Kramer, Large-scale experiments in river hydraulics, *Civ. Eng.*, *2*, 670–674, 1932.

Engelund, F., Hydraulic resistance of alluvial streams, *J. Hydraul. Div. Am. Soc. Civ. Eng.*, *92*, 315–326, 1966.

Everts, C. H., Particle overpassing on flat granular boundaries, *J. Waterw. Harbors Coastal Eng. Div. Am. Soc. Civ. Eng.*, *99*, 425–439, 1973.

Fahnestock, R. K., Morphology and hydrology of a glacial stream—White River, Mount Rainier, Washington, *U.S. Geol. Surv. Prof. Pap. 422A*, 70 pp., 1963.

Fenton, J. D., and J. E. Abbott, Initial movement of grains on a stream bed: The effect of relative protrusion, *Proc. R. Soc. London A*, *352*, 523–537, 1977.

Ferguson, R. I., Critical discharge for entrainment of poorly sorted gravel, *Earth Surf. Processes Landforms*, *19*, 179–186, 1994.

Ferguson, R. I., K. L. Prestegaard, and P. J. Ashworth, Influence of sand on hydraulics and gravel transport in a braided gravel bed river, *Water Resour. Res.*, *25*, 635–643, 1989.

Fernandez Luque, R., and R. van Beek, Erosion and transport of bed-load sediment, *J. Hydraul. Res.*, *14*, 127–144, 1976.

Flintham, T. P., and P. A. Carling, The prediction of mean bed and wall boundary shear in uniform and compositely rough channels, in *International Conference on River Regime*, edited by W. R. White, pp. 267–287, John Wiley, New York, 1988.

Folk, R. L., *Petrology of Sedimentary Rocks*, 182 pp., Hemphill Publ., Austin, Tex., 1974.

Fripp, J. B., and P. Diplas, Surface sampling in gravel streams, *J. Hydraul. Eng.*, *119*, 473–490, 1993.

Gessler, J., Beginning and ceasing of sediment motion, in *River Me-*

chanics, edited by H. W. Shen, pp. 7:1–7:22, H. W. Shen, Fort Collins, Colo., 1971.

Gilbert, G. K., The transportation of débris by running water, *U.S. Geol. Surv. Prof. Pap. 86*, 263 pp., 1914.

Gomez, B., and M. Church, An assessment of bed load sediment transport formulae for gravel bed rivers, *Water Resour. Res.*, *25*, 1161–1186, 1989.

Grass, A. J., Initial instability of fine bed sand, *J. Hydraul. Div. Am. Soc. Civ. Eng.*, *96*, 619–632, 1970.

Griffiths, G. A., Form resistance in gravel channels with mobile beds, *J. Hydraul. Eng.*, *115*, 340–355, 1989.

Guy, H. P., D. B. Simons, and E. V. Richardson, Summary of alluvial channel data from flume experiments, 1956–61, *U.S. Geol. Surv. Prof. Pap. 462-I*, 96 pp., 1966.

Hammond, F. D. C., A. D. Heathershaw, and D. N. Langhorne, A comparison between Shields' threshold criterion and the movement of loosely packed gravel in a tidal channel, *Sedimentology*, *31*, 51–62, 1984.

Hey, R. D., Flow resistance in gravel-bed rivers, *J. Hydraul. Div. Am. Soc. Civ. Eng.*, *105*, 365–379, 1979.

Hey, R. D., Bar form resistance in gravel-bed rivers, *J. Hydraul. Eng.*, *114*, 1498–1508, 1988.

Ho, C., Determination of bottom velocity necessary to start erosion in sand, Ph.D. dissertation, Univ. of Iowa, Iowa City, 1933.

Ho, P.-Y., Abhangigkeit der geschiebebewegung von der kornform und der temperatur, *Mitt. Preuss. Versuchsanst. Wasserbau Erdbau Schiffbau*, *37*, 43, 1939.

Ikeda, S., Incipient motion of sand particles on side slopes, *J. Hydraul. Div. Am. Soc. Civ. Eng.*, *108*, 95–114, 1982.

Ippen, A. T., and R. P. Verma, The motion of discrete particles along the bed of a turbulent stream, in *Proceedings of the Minnesota International Hydraulics Convention*, pp. 7–20, Int. Assoc. Hydraul. Res., Delft, Netherlands, 1953.

James, C. S., Prediction of entrainment conditions for nonuniform noncohesive sediments, *J. Hydraul. Res.*, *28*, 25–41, 1990.

Jiang, Z., and P. K. Haff, Multiparticle simulation methods applied to the micromechanics of bed load transport, *Water Resour. Res.*, *29*, 399–412, 1993.

Johnson, J. W., The importance of considering side-wall friction in bed-load investigations, *Civ. Eng.*, *12*, 329–331, 1942.

Johnson, J. W., Laboratory investigations on bed-load transportation and bed roughness, a compilation of published and unpublished data, *U.S. Dep. Agric. Soil Cons. Serv. SCS-TP-50*, 116 pp., 1943.

Jorissen, A. L., Étude expérimentale du transport solide des cours d'eau, *Rev. Univ. Mines*, *14*, 269–282, 1938.

Kamphuis, J. W., Determination of sand roughness for fixed beds, *J. Hydraul. Res.*, *12*, 193–203, 1974.

Kellerhals, R., and D. I. Bray, Sampling procedures for coarse fluvial sediments, *J. Hydraul. Div. Am. Soc. Civ. Eng.*, *97*, 1165–1180, 1971.

Kinerson, D., Bed surface response to sediment supply, M.S. thesis, 420 pp., Univ. of Calif., Berkeley, 1990.

Kirchner, J. W., W. E. Dietrich, F. Iseya, and H. Ikeda, The variability of critical shear stress, friction angle, and grain protrusion in water worked sediments, *Sedimentology*, *37*, 647–672, 1990.

Knight, D. G., Boundary shear in smooth and rough channels, *J. Hydraul. Div. Am. Soc. Civ. Eng.*, *107*, 839–851, 1981.

Komar, P. D., Selective grain entrainment by a current from a bed of mixed sizes: A reanalysis, *J. Sediment. Petrol.*, *57*, 203–211, 1987a.

Komar, P. D., Selective gravel entrainment and the empirical evaluation of flow competence, *Sedimentology*, *34*, 1165–1176, 1987b.

Komar, P. D., and P. A. Carling, Grain sorting in gravel-bed streams and the choice of particle sizes for flow-competence evaluations, *Sedimentology*, *38*, 489–502, 1991.

Komar, P. D., and S.-M. Shih, Equal mobility versus changing bedload grain sizes in gravel-bed streams, in *Dynamics of Gravel-bed Rivers*, edited by P. Billi, R. D. Hey, C. R. Thorne, and P. Tacconi, pp. 73–106, John Wiley, New York, 1992.

Komar, P. D., and C. Wang, Processes of selective grain transport and the formation of placers on beaches, *J. Geol.*, *95*, 637–655, 1984.

Kondolf, G. M., and P. Wilcock, The flushing flow problem, *Eos Trans. AGU*, *73*, 239, 1992.

Kramer, H., Sand mixtures and sand movement in fluvial models, *Trans. Am. Soc. Civ. Eng.*, *100*, 798–878, 1935.

Kuhnle, R. A., Fractional transport rates of bedload on Goodwin Creek, in *Dynamics of Gravel-bed Rivers*, edited by P. Billi, R. D. Hey, C. R. Thorne, and P. Tacconi, pp. 141–155, John Wiley, New York, 1992.

Kuhnle, R. A., Equal mobility on Goodwin Creek, *Eos Trans. AGU*, *74*, 158, 1993a.

Kuhnle, R. A., Incipient motion of sand-gravel sediment mixtures, *J. Hydraul. Eng.*, *119*, 1400–1415, 1993b.

Kuhnle, R. A., and A. J. Bowie, Loop rating curves from Goodwin Creek, in *Hydraulic Engineering '92*, edited by M. Jennings and N. G. Bhowmik, pp. 741–746, Am. Soc. Civ. Eng., New York, 1992.

Lane, E. W., Design of stable channels, *Trans. Am. Soc. Civ. Eng.*, *120*, 1234–1279, 1955.

Lavelle, J. W., and H. O. Mofjeld, Do critical stresses for incipient motion and erosion really exist?, *J. Hydraul. Eng.*, *113*, 370–385, 1987.

Leopold, L. B., and W. W. Emmett, Bedload measurements, East Fork River, Wyoming, *Proc. Natl. Acad. Sci. U.S.A.*, *73*, 1000–1004, 1976.

Leopold, L. B., and W. W. Emmett, 1976 bedload measurements, East Fork River, Wyoming, *Proc. Natl. Acad. Sci. U.S.A.*, *74*, 2644–2648, 1977.

Leopold, L. B., M. G. Wolman, and J. P. Miller, *Fluvial Processes in Geomorphology*, 522 pp., W. H. Freeman, New York, 1964.

Lepp, L. R., C. J. Koger, and J. A. Wheeler, Channel erosion in steep gradient, gravel-paved streams, *Bull. Assoc. Eng. Geol.*, *30*, 443–454, 1993.

Li, M. Z., and P. D. Komar, Laboratory measurements of pivoting angles for applications to selective entrainment of gravel in a current, *Sedimentology*, *33*, 413–423, 1986.

Li, Z., and P. D. Komar, Selective entrainment and transport of mixed size and density sands: Flume experiments simulating the formation of black-sand placers, *J. Sediment. Petrol.*, *62*, 584–590, 1992.

Ling, C.-H., Criteria for incipient motion of spherical sediment particles, *J. Hydraul. Eng.*, *121*, 472–478, 1995.

Liu, T.-Y., Transportation of the bottom load in an open channel, M.S. thesis, 34 pp., Univ. of Iowa, Iowa City, 1935.

MacDougall, C. H., Bed-sediment transportation in open channels, *Eos Trans. AGU*, *14*, 491–495, 1933.

Mantz, P. A., Low transport stages by water streams of fine, cohesionless granular and flaky sediments, Ph.D. dissertation, Univ. of London, London, 1975.

Mantz, P. A., Incipient transport of fine grains and flakes by fluids—Extended Shields diagram, *J. Hydraul. Div. Am. Soc. Civ. Eng.*, *103*, 601–615, 1977.

Mavis, F. T., C. Ho, and Y.-C. Tu, The transportation of detritus by flowing water, I, *Univ. Iowa Studies Eng.*, *5*, 1–53, 1935.

Mavis, F. T., T. Liu, and E. Soucek, The transportation of detritus by flowing water, II, *Univ. Iowa Studies Eng.*, *11*, 1–28, 1937.

Meland, N., and J. O. Norrman, Transport velocities of single particles in bed-load motion, *Geogr. Ann.*, *48A*, 165–182, 1966.

Meland, N., and J. O. Norrman, Transport velocities of individual size fractions in heterogeneous bed load, *Geogr. Ann.*, *51A*, 127–144, 1969.

Meyer-Peter, E., and R. Müller, Formulas for bed-load transport, in *Proceedings of the 2nd Meeting of the International Association for Hydraulic Structures Research*, pp. 39–64, Inter. Assoc. for Hydraul. Res., Delft, Netherlands, 1948.

Middleton, G. V., and J. B. Southard, *Mechanics of Sediment Movement*, 401 pp., Soc. of Econ. Paleontol. and Mineral., Tulsa, Okla., 1984.

Milhous, R. T., Sediment transport in a gravel-bottomed stream, Ph.D. dissertation, 232 pp., Oreg. State Univ., Corvallis, 1973.

Milhous, R. T., The calculation of flushing flows for gravel and cobble bed rivers, in *Hydraulic Engineering, Proceedings of the 1990 National Conference*, vol. 1, edited by H. H. Chang, pp. 598–603, Am. Soc. Civ. Eng., New York, 1990.

Millar, R. G., and M. C. Quick, Flow resistance of high-gradient gravel channels, in *Hydraulic Engineering, '94*, vol. 1, edited by G. V. Controneo and R. R. Rumer, pp. 717–721, Am. Soc. Civ. Eng., New York, 1994.

Miller, R. T., and R. J. Byrne, The angle of repose for a single grain on a fixed rough bed, *Sedimentology*, *6*, 303–314, 1966.

Miller, M. C., I. N. McCave, and P. D. Komar, Threshold of sediment motion under unidirectional currents, *Sedimentology*, *24*, 507–527, 1977.

Misri, R. L., R. J. Garde, and K. G. R. Raju, Bed load transport of coarse nonuniform sediment, *J. Hydraul. Eng.*, *110*, 312–328, 1984.

Mizuyama, T., Bedload transport in steep channels, Ph.D. dissertation, 118 pp., Kyoto Univ., Kyoto, Japan, 1977.

Montgomery, D. R., J. M. Buffington, N. P. Peterson, D. Schuett-Hames, and T. P. Quinn, Streambed scour, egg burial depths and the influence of salmonid spawning on bed surface mobility and embryo survival, *Can. J. Fish. Aquat. Sci.*, *53*, 1061–1070, 1996.

Naden, P., An erosion criterion for gravel-bed rivers, *Earth Surf. Processes Landforms*, *12*, 83–93, 1987.

Neill, C. R., Mean-velocity criterion for scour of coarse uniform bed-material, in *Proceedings of the 12th Congress of the International Association of Hydraulics Research*, vol. 3, pp. 46–54, Inter. Assoc. for Hydraul. Res., Delft, Netherlands, 1967.

Neill, C. R., and M. S. Yalin, Quantitative definition of beginning of bed movement, *J. Hydraul. Div. Am. Soc. Civ. Eng.*, *95*, 585–588, 1969.

Nelson, J. M., and J. D. Smith, Flow in meandering channels with natural topography, in *River Meandering*, *Geophys. Monogr. Ser.*, vol. 12, edited by S. Ikeda and G. Parker, pp. 69–126, AGU, Washington, D. C., 1989.

Nikuradse, J., Strömungsgesetze in rauhen Rohren, *Forschg. Arb. Ing. Wes.*, *361*, 22, 1933. (English translation, Laws of flow in rough pipes, *Tech. Memo. 1292*, Natl. Adv. Comm. for Aeron., Washington, D. C., 1950.)

O'Brien, M. P., and B. D. Rindlaub, The transportation of bed-load by streams, *Eos Trans. AGU*, *15*, 593–603, 1934.

Paintal, A. S., Concept of critical shear stress in loose boundary open channels, *J. Hydraul. Res.*, *9*, 91–113, 1971.

Parker, G., Self-formed straight rivers with equilibrium banks and mobile bed, 2, The gravel river, *J. Fluid Mech.*, *89*, 127–146, 1978.

Parker, G., Surface-based bedload transport relation for gravel rivers, *J. Hydraul. Res.*, *28*, 417–436, 1990.

Parker, G., and P. C. Klingeman, On why gravel bed streams are paved, *Water Resour. Res.*, *18*, 1409–1423, 1982.

Parker, G., and A. W. Peterson, Bar resistance of gravel-bed streams, *J. Hydraul. Div. Am. Soc. Civ. Eng.*, *106*, 1559–1575, 1980.

Parker, G., P. C. Klingeman, and D. G. McLean, Bedload and size distribution in paved gravel-bed streams, *J. Hydraul. Div. Am. Soc. Civ. Eng.*, *108*, 544–571, 1982.

Pazis, G. C., and W. H. Graf, Weak sediment transport, *J. Hydraul. Div. Am. Soc. Civ. Eng.*, *103*, 799–802, 1977.

Petit, F., The evaluation of grain shear stress from experiments in a pebble-bedded flume, *Earth Surf. Processes Landforms*, *14*, 499–508, 1989.

Petit, F., Evaluation of grain shear stresses required to initiate movement of particles in natural rivers, *Earth Surf. Processes Landforms*, *15*, 135–148, 1990.

Petit, F., Dimensionless critical shear stress evaluation from flume experiments using different gravel beds, *Earth Surf. Processes Landforms*, *19*, 565–576, 1994.

Powell, D. M., and P. J. Ashworth, Spatial pattern of flow competence and bed load transport in a divided gravel bed river, *Water Resour. Res.*, *31*, 741–752, 1995.

Prager, E. J., J. B. Southard, and E. R. Vivoni-Gallart, Experiments on the entrainment threshold of well-sorted and poorly sorted carbonate sands, *Sedimentology*, *43*, 33–40, 1996.

Prestegaard, K. L., Bar resistance in gravel bed steams at bankfull stage, *Water Resour. Res.*, *19*, 473–476, 1983.

Rathburn, R. E., and H. P. Guy, Measurement of hydraulic and sediment transport variables in a small recirculating flume, *Water Resour. Res.*, *3*, 107–122, 1967.

Raudkivi, A. J., Study of sediment ripple formation, *J. Hydraul. Div. Am. Soc. Civ. Eng.*, *89*, 15–33, 1963.

Reid, I., L. E. Frostick, and J. T. Layman, The incidence and nature of bedload transport during flood flows in coarse-grained alluvial channels, *Earth Surf. Processes Landforms*, *10*, 33–44, 1985.

Robert, A., Boundary roughness in coarse-grained channels, *Prog. Phys. Geog.*, *14*, 42–70, 1990.

Rouse, H., Discussion of "Laboratory investigation of flume traction and transportation," *Trans. Am. Soc. Civ. Eng.*, *104*, 1303–1308, 1939.

Schaffernak, F., Die Ausbildung von Gleichgewichtsprofilen in geraden Flusstrecken mit Geschiebebett, *Mitt. Versuchsanst. Wasserbau Minist. Offentliche Arb.*, 1916.

Schoklitsch, A., *Über Schleppkraft und Geschibebewegung*, Englemann, Leipzig, Germany, 1914.

Shields, F. D., and C. J. Gippel, Prediction of effects of woody debris removal on flow resistance, *J. Hydraul. Eng.*, *121*, 341–354, 1995.

Shields, A., Anwendung der Aehnlichkeitsmechanik und der Turbulenzforschung auf die Geschiebebewegung, *Mitt. Preuss. Versuchsanst. Wasserbau Schiffbau*, *26*, 26, 1936. (English translation by W. P. Ott and J. C. van Uchelen, 36 pp., U.S. Dep. of Agric. Soil Conser. Serv. Coop. Lab., Calif., Inst. of Technol., Pasadena, 1936.)

Shimizu, Y., Effects of lateral shear stress in open channel flow, *Rep. Civ. Eng. Res. Inst. Publ. 439*, 22 pp., Hokkaido Develop. Bur., River Hydraul. Hydrol. Lab., Sapporo, Japan, 1989.

Smith, J. D., and S. R. McLean, Spatially averaged flow over a wavy surface, *J. Geophys. Res.*, *82*, 1735–1746, 1977.

Sternberg, R. W., Measurements of incipient motion of sediment particles in the marine environment, *Marine Geol.*, *10*, 113–119, 1971.

Thompson, S. M., and P. L. Campbell, Hydraulics of a large channel paved with boulders, *J. Hydraul. Res.*, *17*, 341–354, 1979.

Tison, L. J., Recherches sur la tension limite d'entrainment des materiaux constitutifs du lit, in *Proceedings of the Minnesota International Hydraulics Convention*, pp. 21–35, Inter. Assoc. Hydraul. Res., Delft, Netherlands, 1953.

Todd, F. H., Tables of coefficients for A.T.T.C. and I.T.T.C. model ship correlation and kinematic viscosity and density of fresh and salt water, *Tech. Res. Bull. 1-25*, 36 pp., Soc. Nav. Architects Marine Eng., New York, 1964.

Torri, D., and J. Poesen, Incipient motion conditions for single rock fragments in simulated rill flow, *Earth Surf. Processes Landforms*, *13*, 225–237, 1988.

U.S. Waterways Experimental Station (USWES), Study of river-bed material and their use with special reference to the Lower Mississippi River, *Pap. 17*, 161 pp., Vicksburg, Miss., 1935.

Vanoni, V. A., Measurements of critical shear stress for entraining fine sediments in a boundary layer, *KH-R-7*, 47 pp., W. M. Keck Lab., Hydraul. Water Resour. Div. Eng. Appl. Sci., Calif. Inst. of Technol., Pasadena, 1964.

Vanoni, V. A., and N. H. Brooks, Laboratory studies of the roughness and suspended load of alluvial streams, *Sediment. Lab. Rep. E68*, 121 pp., Calif. Inst. of Technol., Pasadena, 1957.

Vanoni, V. A., P. C. Benedict, D. C. Bondurant, J. E. McKee, R. F. Piest, and J. Smallshaw, Sediment transportation mechanics: Initiation of motion, *J. Hydraul. Div. Am. Soc. Civ. Eng.*, *92*, 291–314, 1966.

Ward, B. D., Surface shear at incipient motion of uniform sands, Ph.D. dissertation, 88 pp., Univ. of Ariz., Tucson, 1968.

Wathen, S. J., R. I. Ferguson, T. B. Hoey, and A. Werritty, Unequal mobility of gravel and sand in weakly bimodal river sediments, *Water Resour. Res.*, *31*, 2087–2096, 1995.

White, C. M., The equilibrium of grains on the bed of a stream, *Proc. R. Soc. London A*, *174*, 322–338, 1940.

White, S. J., Plane bed thresholds of fine grained sediments, *Nature*, *228*, 152–153, 1970.

Whiting, P. J., and W. E. Dietrich, Boundary shear stress and roughness over mobile alluvial beds, *J. Hydraul. Eng.*, *116*, 1495–1511, 1990.

Wiberg, P. L., and J. D. Smith, Calculations of the critical shear stress for motion of uniform and heterogeneous sediments, *Water Resour. Res.*, *23*, 1471–1480, 1987.

Wilcock, P. R., Bed-load transport of mixed-size sediment, Ph.D. dissertation, 205 pp., Mass. Inst. of Technol., Cambridge, 1987.

Wilcock, P. R., Methods for estimating the critical shear stress of individual fractions in mixed-size sediment, *Water Resour. Res.*, *24*, 1127–1135, 1988.

Wilcock, P. R., Experimental investigation of the effect of mixture properties on transport dynamics, in *Dynamics of Gravel-bed Rivers*, edited by P. Billi, R. D. Hey, C. R. Thorne, and P. Tacconi, pp. 109–139, John Wiley, New York, 1992a.

Wilcock, P. R., Flow competence: A criticism of a classic concept, *Earth Surf. Processes Landforms*, *17*, 289–298, 1992b.

Wilcock, P. R., Critical shear stress of natural sediments, *J. Hydraul. Eng.*, *119*, 491–505, 1993.

Wilcock, P. R., and B. W. McArdell, Surface-based fractional transport rates: Mobilization thresholds and partial transport of a sand-gravel sediment, *Water Resour. Res.*, *29*, 1297–1312, 1993.

Wilcock, P. R., and J. B. Southard, Experimental study of incipient motion in mixed-size sediment, *Water Resour. Res.*, *24*, 1137–1151, 1988.

Wilcock, P. R., and J. B. Southard, Bed-load transport of mixed-size

sediment: Fractional transport rates, bed forms, and the development of a coarse bed-surface layer, *Water Resour. Res.*, *25*, 1629–1641, 1989.

Wilcock, P. R., A. Barta, C. C. Shea, G. M. Kondolf, W. V. G. Matthews, and J. Pitlick, Observations of flow and sediment entrainment on a large gravel-bed river, *Water Resour. Res.*, *32*, 2897–2909, 1996.

Williams, G. P., Flume width and water depth effects in sediment-transport experiments, *U.S. Geol. Surv. Prof. Pap. 562-H*, 37 pp., 1970.

Wimbush, M., and B. Lesht, Current-induced sediment movement in the deep Florida Straits: Critical parameters, *J. Geophys. Res.*, *84*, 2495–2502, 1979.

Wolman, M. G., and L. M. Brush, Factors controlling the size and shape of stream channels in coarse noncohesive sands, *U.S. Geol. Surv. Prof. Pap. 282-G*, 37 pp., 1961.

Yalin, M. S., *Mechanics of Sediment Transport*, Pergamon, Tarrytown, N. Y., 1977.

Yalin, M. S., and E. Karahan, Inception of sediment transport, *J. Hydraul. Div. Am. Soc. Civ. Eng.*, *105*, 1433–1443, 1979.

Young, R. A., and R. Mann, Erosion velocities of skeletal carbonate sands, St. Thomas, Virgin Islands, *Marine Geol.*, *69*, 171–185, 1985.

J. M. Buffington and D. R. Montgomery, Department of Geological Sciences, University of Washington, Box 351310, Seattle, WA 98195. (e-mail: jbuff@u.washington.edu)

(Received April 17, 1996; revised August 9, 1996; accepted October 18, 1996.)

Correction to "A systematic analysis of eight decades of incipient motion studies, with special reference to gravel-bedded rivers" by John M. Buffington and David R. Montgomery

In the paper "A systematic analysis of eight decades of incipient motion studies, with special reference to gravel-bedded rivers" by John M. Buffington and David R. Montgomery (*Water Resources Research*, *33*(8), 1993–2029, 1997), the symbol for channel slope (S) was incorrectly typeset as a subscript in the equation in the footnote keyed to ‡, Table 1a. The correct equation is

$$h_c = \tau_c^*(\rho_s - \rho) D_{50}/\rho S$$

The authors also would like to point out that their data compilation does not include dimensionless shear stress values that are averages of multiple data sets (e.g., *Meyer-Peter and Müller*'s [1948] $\tau^*_{c_{r50m}} = 0.047$ and *Andrew*'s [1983] $\tau^*_{c_{q50ss}} = 0.083$), as there is no unique critical boundary Reynolds number (Re^*_c) for these values because they combine a range of median grain sizes and boundary roughness conditions. For example, the *Meyer-Peter and Müller* [1948] Shields parameter of 0.047 is based on mixture median grain sizes of 0.4–28.7 mm, corresponding with Re^*_c values ranging from approximately 5 to 3300, effectively spanning the range of boundary Reynolds numbers reported for most Shields curves. Consequently, their Shields parameter of 0.047 can be thought of as an average of an entire Shields curve. In this example, Re^*_c values were estimated as described in the footnote keyed to †, Table 1a, with $\nu = 1.3 \times 10^{-6}$ m^2/s, $D_{50m} = 0.4$–28.7 mm, $\tau^*_{c_{r50m}} = 0.047$, and $\rho_s = 2680$ kg/m^3 [*Meyer-Peter and Müller*, 1948].

Copyright 1998 by the American Geophysical Union.

Paper number 97WR03138.
0043-1397/98/97WR-03138$09.00

References

Andrews, E. D., Entrainment of gravel from naturally sorted riverbed material, *Geol. Soc. Am. Bull.*, *94*, 1225–1231, 1983.

Meyer-Peter, E., and R. Müller, Formulas for bed-load transport, in *Proceedings of the 2nd Meeting of the International Association for Hydraulic Structures Research*, pp. 39–64, Inter. Assoc. for Hydraul. Res., Delft, Netherlands, 1948.

(Received November 4, 1997.)